Copy No. 26

DEFENCE R&D DÉFENSE

First-Ply Failure Prediction of Fibrous Composites with Finite Element Analysis

M.J. Smith
DREA

Defence R&D Canada

Technical Memorandum
DREA TM 2001-065
June 2001

National Defence Défense nationale

Canada

102-02658/

First-Ply Failure Prediction of Fibrous Composites with Finite Element Analysis

M. J. Smith
DREA

Defence Research Establishment Atlantic

Technical Memorandum

DREA TM 2001-065

June 2001

Author

M. J. Smith

Approved by

J. L. Kennedy
Head/Warship Signatures and Safety

Approved for release by

K. Foster
Chair/Document Review Panel

© Her Majesty the Queen as represented by the Minister of National Defence, 2001

© Sa majesté la reine, représentée par le ministre de la Défense nationale, 2001

Abstract

The usefulness of macroscopic failure theories for laminated composites is investigated by means of a finite element based approach for determining first-ply failure loads of structures. A review of phenomenological (macroscopic) failure theories is provided, with detailed descriptions of six stress-based theories. The computational approach for first-ply failure analysis uses a linear static finite element analysis, followed by the iterative scaling of the stress-strain results to satisfy the chosen failure criterion. The resulting scaling factor defines the failure load. The first-ply algorithm and failure criteria have been implemented in a special-purpose finite element code for laminated plate and shell structures. Failure loads are predicted and validated with the six selected stress-based criteria for a rectangular composite plate structure with normal and in-plane loading. The effect of the stress concentration produced by a circular hole is then considered for the in-plane loading case. The strength of angle-ply laminates, both with and without a stress concentration, is then examined as a function of the ply angle. Although no one criterion stands out as superior to the others, good consistency is obtained by four out of the six criteria in predicting failure loads and locations. Among these four, the Maximum Stress and Tsai Wu criteria showed a tendency to over-predict the failure loads, especially with angle-ply laminates. The most consistently performing criteria in the examples tested were the Hoffman and Hashin criteria.

Résumé

On a étudié la pertinence de certaines théories de la rupture macroscopique de composites stratifiés en utilisant une méthode basée sur les éléments finis pour déterminer les charges de rupture du pli élémentaire de structures données. Le présent rapport contient un examen des théories de la rupture phénoménale (macroscopique) et des descriptions détaillées de six théories basées sur les contraintes. Pour analyser la rupture du pli élémentaire, la méthode computationnelle utilise d'abord l'analyse linéaire statique par éléments finis, puis une mise à l'échelle itérative des résultats de contrainte-déformation afin de satisfaire au critère de rupture choisi. Le facteur d'échelle résultant sert à définir la charge de rupture. L'algorithme et le critère de rupture relatifs au pli élémentaire ont été incorporés dans un code d'élément fini spécialisé s'appliquant aux structures de plaques et de coques stratifiées. Les prévisions des charges de rupture, ainsi que leur validation, sont calculées en employant les six critères de rupture choisis, pour le cas d'une structure de plaque composite rectangulaire soumise à une charge normale et dans le plan. On tient aussi compte des effets de la concentration de contraintes qu'entraîne un trou

circulaire, pour une charge dans le plan. On observe ensuite le comportement de la résistance des stratifiées à pli angulaire en fonction de l'angle du pli, en présence et en absence de la concentration de contraintes. Bien qu'aucun critère ne soit supérieur aux autres, on obtient toutefois des résultats ayant un degré de cohérence satisfaisant pour quatre des six critères, pour les prévisions des charges de rupture et les endroits où se produisent les ruptures. Parmi ces quatre critères, ceux dits « Maximum Stress » et « Tsai-Wu » ont tendance à surévaluer les prévisions de charges de rupture, surtout dans le cas des stratifiés à pli angulaire. Les deux critères produisant les résultats les plus cohérents pour les essais en question sont ceux dits « Hoffman » et « Hashin ».

Executive summary

Background

Fibre-reinforced plastic (FRP) composites are finding increased application in naval structures and platforms, due primarily to their superior strength-to-weight ratio and resistance to corrosion. With the possibility of a composite mast re-fit of part of the Canadian Forces' fleet of HALIFAX class frigates, DREA is upgrading its composite structure modelling and analysis capabilities. Central to this effort is a specialised software tool for rapid finite element modelling of warship masts (MAST-SAS) which is currently being developed by Martec Limited of HALIFAX under contract to DREA. Concurrent to this effort, DREA has acquired the commercial finite element analysis software (ANSYS), and is developing a specialised in-house finite element solver for composite plate and shell structures (FELAM).

The yielding/failure behaviour of FRPs is very different from, and very much more complicated than, ductile metals. The combination of strong, stiff fibres with weak, soft resin produces a material with a high degree of anisotropy. Moreover, the presence of small defects in the fibre, matrix (resin), and the fibre-matrix interface, can greatly affect the overall strength of the material. For more than three decades a group of relatively simple failure theories have been used to characterise and predict failure loads for composite materials. This study assesses the usefulness of these theories in the context of finite element analysis (FEA) of laminated composite structures.

Principal Results

Six stress-based failure theories have been included in DREA's FELAM software for FEA of composite plate and shell structures. The six criteria are used in this study to predict first-ply failure loads for a variety of composite laminates. Numerical prediction of the failure load, and the location and mode of failure are compared on a rectangular plate with different loadings and material properties.

As has been found in previous studies of this class of failure theories, no one theory of the six that have been tested stands out as superior to the others. A generally high degree of consistency is obtained with four of the six theories, while anomalous results are obtained with the other two.

Significance of Results

The ability to predict failure loads accurately for composites reduces the amount of structural testing that has to be performed, and this in turns lowers costs. The accuracy of the failure theories at a single-ply level has been established in previous studies on this subject. Application of the theories to laminates and their use in FEA is straight forward, and the generally good level of consistency in the predicted failure loads suggests that the implementation has been successful. Nonetheless questions remain as to the ability of stress-based macroscopic failure theories to accurately predict failures due to their reliance on unrealistic stress quantities and due to the complexity of the failure modes in the matrix.

Future Work

Subsequent investigation of this topic is planned in several areas. The use of strain-based failure criteria and experimental results from the open literature may provide a better base of comparison for assessing the effectiveness of the criteria presented here. Also of interest is failure prediction of sandwich panels typical of marine structures, but these will require a methodology different from the "first-ply" approach considered in this study.

M. J. Smith; 2001; First-Ply Failure Prediction of Fibrous Composites with Finite Element Analysis; DREA TM 2001-065; Defence Research Establishment Atlantic.

Sommaire

Contexte

L'accroissement des applications des composites en plastique renforcé de fibre de verre (PRF) dans les structures et plates-formes marines découle en grande partie des caractéristiques supérieures de ces matériaux au point de vue du rapport résistance-masse et de la résistance à la corrosion. Puisqu'il est possible que des mats en composite remplacent ceux de certaines frégates de la classe HALIFAX de la flotte des Forces canadiennes, le CRDA améliore présentement ses capacités d'analyse et de modélisation de structures de composites. L'outil essentiel à ces travaux est un logiciel spécialisé (MASTSAS) permettant d'effectuer la modélisation rapide par éléments finis de mâts de navires de guerre. L'élaboration du MASTSAS pour le CRDA est actuellement réalisée à l'entreprise, par la société Martec Limited d'Halifax. Simultanément, le CRDA a fait l'acquisition du logiciel commercial ANSYS, pour l'analyse par éléments finis, et il élabore aussi, à l'interne, un résolveur d'éléments finis (FELAM) pour les structures de plaques et de coques composites.

Le comportement des PRF, en matière de limite élastique et de rupture, diffère sensiblement de celui des métaux ductiles et il est beaucoup plus complexe. La combinaison de fortes fibres rigides et d'une résine molle peu résistante donne un matériau ayant un fort degré d'anisotropie. De plus, la présence de légers défauts dans la fibre et la matrice (la résine), ou à l'interface fibre-matrice, peut avoir des répercussions importantes sur la résistance globale du matériau. Depuis plus de 30 ans, on effectue la caractérisation et la prévision des charges de rupture de matériaux composites à l'aide d'un ensemble de théories de la rupture assez simplifiées. La présente étude évalue la pertinence de ces théories par rapport à l'analyse par éléments finis (AEF) de structures de composites stratifiés.

Principaux résultats

On a incorporé six théories de la rupture basées sur la contrainte au logiciel FELAM, élaboré au CRDA, qui permet d'effectuer l'AEF de structures de plaques et de coques composites. Dans la présente étude, les six critères de rupture sont utilisés pour prévoir les charges de rupture du pli élémentaire pour différents composites stratifiés. La comparaison des résultats, pour les prévisions numériques de la charge de rupture, ainsi que pour la nature et l'emplacement de la rupture, est faite pour les cas d'une plaque rectangulaire, composée de matériaux ayant des propriétés différentes, et soumise à des charges de diverses valeurs.

Comme les résultats d'études antérieures sur ce type de théories de la rupture

l'avaient déjà démontré, il n'existe pas une théorie supérieure parmi les six mises à l'essai. On obtient des résultats ayant un degré de cohérence généralement élevé dans le cas de quatre des théories et des résultats anomaux pour les deux autres.

Importance des résultats

La capacité de prévoir avec exactitude les charges de rupture des composites permet de réduire les travaux d'étude des structures sur modèles, ce qui entrane une diminution des cots. Les études antérieures en ce domaine ont bien établi le degré d'exactitude des théories de la rupture, en ce qui concerne le pli élémentaire. L'application des théories aux stratifiés et leur emploi en AEF sont simples et le degré de cohérence des valeurs prévues des charges de rupture est généralement satisfaisant, ce qui suggère une mise en uvre réussie. Il reste toutefois des questions à éclaircir, notamment en ce qui a trait à la capacité des théories de la rupture macroscopique basées sur la contrainte de prévoir les ruptures avec exactitude. Les éléments à considérer sont la dépendance de ces théories et des valeurs de contrainte utilisées, qui sont très peu réalistes, ainsi que le degré de complexité des modes de défaillance se produisant dans la matrice.

Futurs travaux

On prévoit effectuer des études ultérieures portant sur ce sujet dans plusieurs domaines. L'utilisation de critères de rupture basés sur la contrainte et des résultats expérimentaux publiés dans des documents non classifiés pourrait offrir une meilleure base de comparaison pour évaluer l'efficacité des critères de la présente étude. Les prévisions de rupture de panneaux-sandwich, des matériaux typiques de structures marines, constituent aussi un sujet d'intérêt, mais pour les réaliser, il faudra utiliser une méthode différente de l'approche« pli élémentaire» employée dans la présente étude.

M. J. Smith; 2001; Détermination de prévisions de rupture du pli élémentaire de composites fibreux à l'aide de l'analyse par éléments finis ; DREA TM 2001-065; Centre de Recherce pour la Défense Atlantique.

Table of contents

Abstract i

Résumé i

Executive summary iii

Sommaire v

Table of contents vii

List of figures viii

List of tables ix

1 Introduction 1

2 Survey of Failure Theories for Fibrous Composites 3

2.1 Characteristics of Phenomenological Failure Theories 3

2.2 Literature Review 4

2.3 Selected Failure Theories 6

2.3.1 Maximum Stress Criterion 7

2.3.2 Tsai-Hill Criterion 8

2.3.3 Tsai-Wu Criterion 8

2.3.4 Hoffman Criterion 9

2.3.5 Hashin Criterion 9

2.3.6 Christensen Stress Criterion 10

3 Finite Element Methodology 11

3.1 Four-Node Composite Shell Element 11

3.2 Finite Element Stress and Strain Evaluation 11

3.3 First-Ply Failure Load and Location 13

3.4 Implementation 13

4 Numerical Results 16
4.1 Normal Loading 20
4.1.1 Displacement Validation 20
4.1.2 Failure Loads and Locations 20
4.1.3 Effect of Layer Sequence 27
4.2 In-Plane Loading 27
4.3 Angle-Ply Laminates 30
5 Summary and Concluding Remarks 40
References 42
List of symbols, abbreviations, acronyms and initialisms 44
Annex 45
A Sample Felam Model File 45

List of figures

1 Typical FRP layer with unidirectional fibres showing the fibre-matrix co-ordinate system. 6
2 Gauss point positions for the Shell4 element 12
3 Algorithm for Determining First-Ply Failure Load 14
4 Architecture of the Felam Program 15
5 Hierarchy of FELAM Analysis Classes 15
6 Hierarchy of Failure Classes 16
7 Hierarchy of Material Classes 17
8 9×5in Simply-Supported Plate Model 17
9 Symmetric Quarter-Plate Model Used for Cross-Ply Laminates. 19

10 Anti-Symmetric Quarter-Plate Model Used for Angle-Ply Laminates. . 19

11 Element Numbering Scheme for Symmetric Plate Models. 21

12 Element Numbering Scheme for Full Plate Models. 21

13 Effect of Lay-Up Sequence on First-Ply Normal Failure Load of Gr-Ep Laminates. 27

14 Effect of Lay-Up Sequence on First-Ply Normal Failure Load with Fibreglass Laminates. 28

15 9x5 Plate Model with Hole and In-Plane Uniaxial Loading 28

16 Mesh for 9x5 Plate Models with Circular Hole (All Laminates). Failure Locations Predicted for the Nine Laminates Are Shown. 29

17 Failure Load Ratios (Failure Load with Hole / Failure Load without Hole) for In-Plane Loading of Graphite Epoxy Laminates. 34

18 Failure Loads Per Layer for In-Plane Loading of Graphite Epoxy Laminates with a Circular Hole. 35

19 Failure Load Ratios (Failure Load with Hole / Failure Load without Hole) for In-Plane Loading of Fibreglass Laminates. 36

20 Failure Loads Per Layer for In-Plane Loading of Fibreglass Laminates with a Circular Hole. 37

21 Failure Loads as a Function of Ply Angle for a Uniform Plate with Two Angle-Ply Graphite Epoxy Laminates. 38

22 Failure Loads as a Function of Ply Angle for a Plate with a Hole and with Two Angle-Ply Graphite Epoxy Laminates. 39

23 Failure Loads as a Function of Ply Angle for a Uniform Plate with Two Angle-Ply Fibreglass Laminates. 39

24 Failure Loads as a Function of Ply Angle for a Plate with a Hole and with Two Angle-Ply Fibreglass Laminates. 40

List of tables

1 Nine lamination schemes used in the plate model analysis [23]. 18

2 Material properties for T300/5208 graphite epoxy. 18

3 Material Properties for Fibreglass. 19

4 Analytical and FE Maximum Deflections for Uniform Pressure Loading of a 9x5 Plate Model. 20

5 First-Ply Failure for Uniform Pressure Loading of Laminate A. 23

6 First-Ply Failure for Uniform Pressure Loading of Laminate B. 23

7 First-Ply Failure for Uniform Pressure Loading of Laminate C. 23

8 First-Ply Failure for Uniform Pressure Loading of Laminate D. 24

9 First-Ply Failure for Uniform Pressure Loading of Laminate E. 24

10 First-Ply Failure for Uniform Pressure Loading of Laminate F. 24

11 First-Ply Failure for Uniform Pressure Loading of Laminate G. 25

12 First-Ply Failure for Uniform Pressure Loading of Laminate H. 25

13 First-Ply Failure for Uniform Pressure Loading of Laminate I. 25

14 Correlation of Failure Load Results with Reddy and Pandey[23]. . . . 26

15 First-Ply Failure Predicted by ANSYS and FELAM for the Maximum Stress Criterion. 26

16 First-Ply Failure for In-Plane Loading of Laminate A with Hole. 30

17 First-Ply Failure for In-Plane Loading of Laminate B with Hole. 31

18 First-Ply Failure for In-Plane Loading of Laminate C with Hole. 31

19 First-Ply Failure for In-Plane Loading of Laminate D with Hole. 31

20 First-Ply Failure for In-Plane Loading of Laminate E with Hole. 32

21 First-Ply Failure for In-Plane Loading of Laminate F with Hole. 32

22 First-Ply Failure for In-Plane Loading of Laminate G with Hole. 32

23 First-Ply Failure for In-Plane Loading of Laminate H with Hole. 33

24 First-Ply Failure for In-Plane Loading of Laminate I with Hole. 33

25 First-Ply Failure Predicted by ANSYS and FELAM for the Maximum Stress Criterion. 33

This page intentionally left blank.

1 Introduction

The mechanisms of failure in fibrous composite materials are considerably more complicated than those encountered in ductile metals. This is the result of combining material types with disparate stiffness and strength properties in an anisotropic arrangement. A typical fibre reinforced polymer (FRP) composite consists of high modulus, high strength, and brittle fibres coupled with a low modulus, low strength, ductile matrix. The kinds of failure that can occur in tension include yielding, fracture, and pull-out of the fibres, as well as yielding and fracture of the matrix. In compression, the fibres may fail due to yielding, kinking, or micro-buckling while the matrix fails due to yielding or fracture. Failure of the fibres can often be attributed to pre-existing kinking, misalignments, and other defects; fracture of the matrix is often the result of pre-existing voids or microcracking. When a composite material is in the form of a laminate consisting of two or more fibrous layers, debonding of the layers (delamination) is also a concern. Considerable variation in the strength of a composite can result from inconsistencies in the fabrication process.

It is impractical to determine the strength of composite structural components solely by experimental means. Some kind of predictive capability is required, whether analytical or numerical in nature, both to reduce the amount of experimental testing and to increase the number of designs and load cases that can be investigated. Methods for predicting strength of composites are generally either micro-mechanical or phenomenological in nature. Micro-mechanical methods range from studies at the molecular level to refined finite element modelling of individual fibres and the surrounding matrix. Micro-mechanical methods include the unit cell method [1], in which a single fibre embedded in a cube of resin is analysed assuming a periodic distribution of fibres, and the multi-continuum method [2], in which the stress-strain properties of the resin and fibres are continually updated throughout a structural analysis. Although strides have been taken in the direction of computationally efficient micro-mechanical methods, most approaches of this type are much too detailed for effective use in structural analysis. Their role is primarily in evaluating the fundamental strength and stiffness properties of particular fibre-resin combinations. An example of such a micro-mechanical study is provided by Skudra [3]. The interest in micro-mechanical studies and the emphasis on testing to establish physical properties of composites is evidence of the skepticism with which simple laws for strength and stiffness properties, such as rule of mixtures (ROM) formulas, are now viewed.

Phenomenological methods are macro-mechanical or macroscopic in nature, in that they treat the combination of fibre and resin as a single, homogenised material with anisotropic properties. These approaches typically establish criteria for failure using the overall stress-strain behaviour of a material without having a detailed un-

derstanding of how the fibres and matrix produce the behaviour. The simplification that comes from using a phenomenological approach makes it suitable for use in the analysis of complex structure. In order to use a phenomenological criterion, the stiffness and strength of the material first have to be determined at the laminar level, either by experimental or micromechanical methods.

This Memorandum discusses the use of phenomenological failure methods in finite element analysis of laminated composite structures. Failure prediction can be carried out on a "first-ply" basis, in which failure is defined to be when a single ply of a laminate undergoes a failure anywhere in the structure. Or it can be carried out on a progressive failure basis, in which failure is defined as an overall loss of strength in the structure. The latter approach recognises that considerable residual strength may exist in a structure that has undergone a first- or multiple-ply failure. The analysis of progressive failure is inherently nonlinear, and can exceedingly complicate a structural analysis. At the design stage, the first-ply approach offers the advantage of computational efficiency, since it can be performed with linear finite element analysis. A progressive failure analysis may be more appropriate at the end of the design cycle, when a viable design has been established using first-ply methods.

This Memorandum uses the first-ply technique as a means of evaluating the effectiveness of phenomenological failure criteria. An algorithm is presented for predicting the failure load, i.e., the load applied in a given loading arrangement that produces a first-ply failure condition, using linear FEA. The algorithm described has been implemented in FELAM, a special-purpose finite element code for laminate plate and shell structures. Examples of failure prediction are provided that involve normal and in-plane loading of laminated plates. Although the emphasis is on laminate structures, the first-ply technique described in this work can be applied to a wider class of structure. By including failure criteria for isotropic materials, e.g., the Tresca and Von Mises criterion, structures with hybrid materials such as composite sandwiches (an isotropic or orthotropic core material between laminated face sheets) can be handled within the first-ply framework. Of course, in doing this it is necessary to use a finite element model appropriate to the physical phenomenon under investigation. The scope of the present study is limited to static failure prediction, and does not consider failure due to fatigue and other long-term service or environmental effects.

2 Survey of Failure Theories for Fibrous Composites

2.1 Characteristics of Phenomenological Failure Theories

A large number and wide variety of phenomenological (macro-mechanical) failure theories have been proposed for fibrous composite materials. Although nearly all have been shown to satisfy some experimental results, no single "best" failure theory has yet been identified which matches measured data for all material types. Extensive reviews of phenomenological failure theories have been given by Rowlands [4], Nahas [5], Echaabi et al [6], and others. A notable feature of these methods is the absence of a physical description of the failure process. Instead, failure is assumed to be of a particular mathematical form (some function of the strains or stresses), with parameters that are left to be determined either from measurements or from micro-mechanical knowledge of the material behaviour.

Composite failure theories usually pertain to individual lamina, but have also been developed for whole laminates. The former is generally preferred, since a failure theory that has been validated for a lamina of given material properties can then be used for all laminates involving that material; whereas in the case of a laminate failure theory a new criterion has to be derived for each new laminate encountered, even if the laminae are all of the same material type. For laminar failure theories, the mathematical form may be strain-based, in which case the strains used are those along the principal material directions of the lamina. Laminar strains in the fibres and resin are assumed to be identical, which is a reasonably good approximation even in cases of very stiff fibres in a soft resin. When the mathematical form is stress-based, the stresses used are neither the fibre stresses nor the resin stresses, but rather a smeared average of the two. The stress averaging results from assuming homogeneous (but anisotropic) material properties throughout each lamina. The use of homogenised stresses eliminates much of the complexity involved in predicting stresses among fibres and the surrounding matrix. But it is open to question whether a meaningful representation of the failure can be obtained with homogenised stresses. One of the purposes of the present study is to answer this question.

The relative merits of strain- versus stress-based theories have been discussed in the literature. Some believe that strain-based theories are better because laminar strains can be determined more directly, whether calculated or measured, and are more accurate than homogenised stresses. But others have noted that laminate deformation usually produces something near a plane stress condition in the laminae, and there-

fore it is more natural to use stress, even homogenised stress, as the basis of the failure criteria. In fact, the majority of existing phenomenological failure theories are stress based.

Failure criteria can be represented graphically as a failure surface in stress or strain space, according to their mathematical form. In the case of stress-based theories, the failure surface is enscribed about the three orthogonal axes σ_{11}, σ_{22}, and τ_{12}. σ_{11} is the normal stress in the fibre direction, σ_{22} is the stress in the direction normal to the fibres in the plane of the laminae, and τ_{12} is the in-plane shear stress. Because plane stress conditions are usually assumed in laminae, the other stress components are neglected as insignificant to the failure mechanics. Instead of presenting the whole failure surface in three dimensions, it is customary to look at failure envelopes generated by intersecting the surface at constant values of τ_{12}. Typically, the failure envelope in the $\tau_{12} = 0$ plane is considered, as most of experimental strength data will occur in this plane. Strain-based theories can be graphically represented in a similar manner using the strain space axes (ϵ_1, ϵ_2, γ_{12}), where ϵ_1 and ϵ_2 are normal strains in the laminar plane and γ_{12} is the in-plane shear strain.

2.2 Literature Review

Early developments in composite failure theories treated the material as being analogous to isotropic materials and anisotropic metals. Apart from the maximum stress (strain) criterion, which today remains as one of the most popular theories due to its simplicity, most of the early composite theories attempted to derive a single polynomial expression for the failure envelope of the material. The Tsai-Hill [7] and Hoffman [8] theories are examples of this approach, and numerous others are discussed in review papers [4, 5, 6]. The polynomial approach to the problem culminated in the Tsai-Wu quadratic tensor-polynomial criteria [9]. This criterion uses a general tensor-polynomial expression, truncated after the second-order terms in stress (or strain). The coefficients of the tensor-polynomial can be directly expressed in terms of the measured strengths of the material.

The Tsai-Wu criterion has become one of the most popular composite failure theories and has now been included in many commerical analysis codes. Its advantages are perceived to be its generality and the simplicity of using a single expression for the failure envelope. But a number of problems have been noted with the Tsai-Wu criterion. First, some of the coupling coefficients are difficult to determine because biaxial tests are required, and because these tests do not yield a unique value of the coefficient. Moreover, the shape of the failure envelope is highly sensitive to small errors in the coupling coefficients. Secondly, the wisdom of attempting to use a single expression, however general it may be, to describe a variety of complex failure mechanisms has been questioned [10]. Attempts have been made to improve

the Tsai-Wu criterion by adding third-order stress terms in the tensor-polynomial, as was done in the work of Tennyson et al. [11]. They concluded that the additional experimental testing required to establish the third-order coefficients was not justified by the modest improvement in accuracy. Pang et al. [12] developed two modified versions of the Tsai-Wu criterion with diminished experimental testing requirements. These eliminated the problem of evaluating the coupling coefficients with biaxial tests, but not without sacrificing the accuracy of failure prediction.

Hashin [13] proposed a completely different kind of failure theory in which micromechanical knowledge was used to derive a series of conditional failure criteria, some of which govern failure in the fibres, and others failure in the matrix. As with the tensor polynomial approach, the coefficients of the conditional criteria would be determined by measured strength values. Together, the conditional failure criteria form a piecewise-continuous failure envelope for the material. Since the appearance of the Hashin criteria, other "piecewise" criteria have been developed by other researchers. Notable among these is the work of Hart-Smith [10, 14], who developed a theory for composite failure based on the maximum shear stress (Tresca) criterion for isotropic materials. In doing so he considered only the failure of the fibres, arguing that failure of the matrix is difficult to predict and in any case is not important, since well-designed laminates should always fail in their fibres. In this approach, the failure envelope of a whole laminate can be determined by rotating, superimposing and truncating the piecewise envelopes of the fibres for each layer. Christensen [15] developed a strain-based piecewise failure theory in which maximum strain theory is used for the fibres and a polynomial function in terms of strain invariants was used for the matrix. Later Christensen [16] developed a stress-based theory in which polynomials in terms of stress invariants were used in separate fibre and matrix criteria. Feng [17] used a single polynomial expression in terms of the strain invariants to described composite failure, but then showed that the polynomial can be broken into two separate expressions, one for the fibres and one for the matrix.

Yeh and Kim [18] developed a piecewise failure theory by applying the Yeh-Stratton criterion for isotropic materials. Their approach was to use a separate Yeh-Stratton failure equation in each quadrant of the failure plane. Each equation contains an unknown coupling coefficient that has to be determined by experiment. Labossiere and Neale [19, 20] proposed a generalised parametric failure theory in which the failure envelope is represented as a Fourier series in stress space. The approach can also be used in a piecewise fashion, by changing the Fourier components from quadrant to quadrant. Makinde et al. [21] developed a similar parametric approach in strain space. The authors show that realistic failure envelopes can be generated by this approach, provided sufficient experimental data is available (including data from biaxial tests). The main drawback with the parametric approach is that considerable work is required to tune the Fourier coefficients to best fit the data. Echaabi

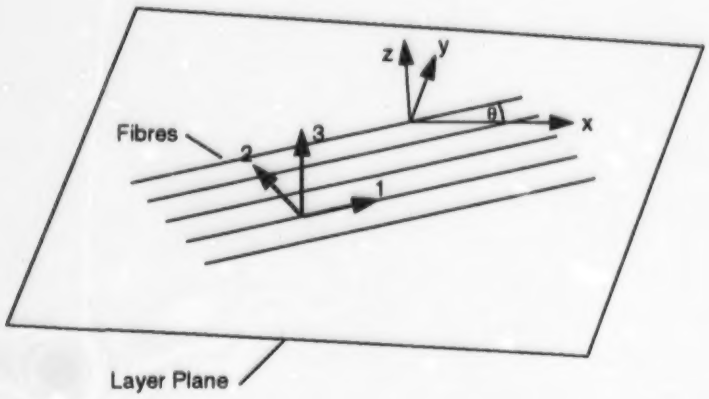

***Figure 1:** Typical FRP layer with unidirectional fibres showing the fibre-matrix co-ordinate system.*

et al. [22] proposed a method for developing a failure envelope by using a statistical fitting method called dual-kriging. In this approach a single failure function is used, but it is supplemented by a large number of terms dependent on the variance of the function from the measured data. By satisfying certain conditions, the failure function can be made to pass through all of the measured data. As with the parametric approach, this approach is beneficial when a substantial amount of bi-axial experimental data is available to fit the curve. With only the measured tensile, compressive and shear strengths in the principal material directions, the parametric and kriging approaches have little advantage over the Tsai-Wu criterion.

The following section presents six selected failure theories in detail. These theories will be applied in numerical examples that appear later in this Memorandum.

2.3 Selected Failure Theories

Although the failure theories being presented here are to be applied to composite laminates under approximately plane stress conditions, it is useful from the point of view of a generalised finite element treatment to present the theories in a fully developed form with all stress and strain components included.

The co-ordinate system for a single ply within a composite laminate is shown in Figure 1. The homogenised stress state in a layer is indicated by $\sigma_1, \sigma_2, \sigma_3, \sigma_4, \sigma_5, \sigma_6$, where the stresses are for the 11, 22, 33, 12, 13, and 23 directional components, respectively. In a unidirectional fibre layer, direction 1 is the fibre direction, direction 2 is perpendicular to the fibres in the plane of the layer, and direction 3 is perpendicular to the layer. Similarly $\epsilon_1, \epsilon_2, \epsilon_3, \epsilon_4, \epsilon_5, \epsilon_6$, are the laminar strains.

Laminar strengths are indicated by $S_1^+, S_1^-, S_2^+, S_2^-, S_3^+, S_3^-, S_4, S_5, S_6$, where the numerical subscripts are the same as for stresses, and where + and − indicate tensile and compressive normal strengths, respectively. Tensile strengths are assumed to be positive; compressive strengths are assumed to be negative. No sign distinction is required for shear strengths. Similarly, $s_1^+, s_1^-, s_2^+, s_2^-, s_3^+, s_3^-, s_4, s_5, s_6$ are used to indicate the laminar strain limits.

Many stress-based failure criteria can be expressed in a tensor polynomial form, the most general form of which is given by

$$F_i\sigma_i + F_{ij}\sigma_i\sigma_j + F_{ijk}\sigma_i\sigma_j\sigma_k + \cdots \geq 1 \tag{1}$$

The unknown coefficients $F_i, F_{ij}, F_{ijk}, \ldots$ are evaluated by means of a series of specialised strength tests performed on single-ply coupons of a material. Each test isolates particular terms in the inequality. By performing a sufficient number of tests, enough equations will be obtained to solve for the coefficients. The homogenised stress components are obtained from the failure load and the dimensions of the coupon. Some of the coefficients are more difficult to determine than others. Many more tests are required to obtain the third-order coefficients than just the first and second-order coefficients. For this reason, the general tensor-polynomial expression is usually truncated after the second-order terms. The second-order coupling terms $F_{ij}, i \neq j$, require bi-axial tests for indentification. These tests are difficult to perform and do not lead to a unique result for F_{ij}. This has produced some uncertainty as to how to properly use failure criteria that make use of the coupling terms in (1).

Satisfaction of (1) indicates that failure has occurred. A failure index can be defined by the nearness of a given stress state is to a failure condition. This can be determined by attaching a common multiplier to the stress vector $\overline{\sigma} = s\sigma$. By replacing σ with $\overline{\sigma}$, the failure equation can then be solved for the multiplier s. The quantity $1/s$ then defines the failure index. The failure load is obtained by multiplying the existing load by the multiplier s, as will be described in Section 3.

2.3.1 Maximum Stress Criterion

This is an independent failure criterion in which each stress component is compared with its corresponding strength component. This is expressed as

$$\begin{array}{lll} \sigma_1 \geq S_1^+ & \sigma_1 \leq S_1^- & |\sigma_4| \geq S_4 \\ \sigma_2 \geq S_2^+ & \sigma_2 \leq S_2^- & |\sigma_5| \geq S_5 \\ \sigma_3 \geq S_3^+ & \sigma_3 \leq S_3^- & |\sigma_6| \geq S_6 \end{array} \tag{2}$$

Failure is indicated by any one of the inequalities being satisfied.

2.3.2 Tsai-Hill Criterion

This criterion came about by assuming that the failure criterion for a unidirectional FRP material has the same mathematical form as an orthotropic, ideally plastic material. This latter is given by

$$A(\sigma_1 - \sigma_2)^2 + B(\sigma_2 - \sigma_3)^2 + C(\sigma_3 - \sigma_1)^2 + 2D\sigma_4^2 + 2E\sigma_5^2 + 2F\sigma_6^2 \geq 1$$

This form has an advantage in that coefficients A through F can be readily determined from simple tests. But note that the normal stresses only appear as the squares of their differences, which implies that this criterion will be unaffected by the presence of an isotropic stress. While this assumption may be valid for isotropic metals, it is not valid for fibre composites, e.g., consider isotropic tension in a composite with unidirectional fibres [13].

The above mathematical form can be re-arranged as follows

$$\begin{aligned}(\sigma_i/S_i)^2 - &\left(1/S_1^2 + 1/S_2^2 - 1/S_3^2\right)\sigma_1\sigma_2 \\ - &\left(1/S_2^2 + 1/S_3^2 - 1/S_1^2\right)\sigma_2\sigma_3 \\ - &\left(1/S_3^2 + 1/S_1^2 - 1/S_2^2\right)\sigma_3\sigma_2 \geq 1 \end{aligned} \tag{3}$$

A summation of terms is implied by the repeated indices in the first term. In (3) S_1, S_2, S_3 are taken to be S_1^+, S_2^+, S_3^+ or S_1^-, S_2^-, S_3^-, according to the signs of the stresses $\sigma_1, \sigma_2, \sigma_3$, respectively.

2.3.3 Tsai-Wu Criterion

This criterion was developed by assuming a second-order polynomial expression of the tensor-polynomial form (1):

$$F_i\sigma_i + F_{ij}\sigma_i\sigma_j \geq 1 \tag{4}$$

The coefficients are determined by performing suitable tests with known stress components at failure. These have been evaluated as follows:

$$F_1 = \frac{1}{S_1^+ - S_1^-}; \qquad F_2 = \frac{1}{S_2^+ - S_2^-}; \qquad F_3 = \frac{1}{S_3^+ - S_3^-};$$

$$F_{11} = \frac{1}{S_1^+ S_1^-}; \qquad F_{22} = \frac{1}{S_2^+ S_2^-}; \qquad F_{33} = \frac{1}{S_3^+ S_3^-};$$

$$F_{44} = \frac{1}{S_4^2}; \qquad F_{55} = \frac{1}{S_5^2}; \qquad F_{66} = \frac{1}{S_6^2};$$

$$F_{12} = -1/2\sqrt{S_1^+ S_1^- S_2^+ S_2^-}; \qquad F_{13} = -1/2\sqrt{S_1^+ S_1^- S_3^+ S_3^-};$$

$$F_{23} = -1/2\sqrt{S_2^+ S_3^- S_3^+ S_3^-};$$

with all other coefficients being zero. Note that linear stress terms have been included so that isotropic stress will have an effect on the predicted failure. Also note that no linear terms in shear stress remain, nor any second order coupling terms in the shear stresses. This is a consequence of material failures being insensitive to sign changes in shear stresses. Thus all terms must vanish in which a given shear stress component appears in the first power.

2.3.4 Hoffman Criterion

The Hoffman criterion is an attempt to improve the Tsai-Hill criterion by adding terms linear in the normal stresses. Rearranging the terms gives the following inequality:

$$\begin{aligned}
&\frac{1}{2}\left(\frac{1}{S_2^+ S_2^-}+\frac{1}{S_3^+ S_3^-}-\frac{1}{S_1^+ S_1^-}\right)(\sigma_2-\sigma_3)^2+\\
&\frac{1}{2}\left(\frac{1}{S_3^+ S_3^-}+\frac{1}{S_1^+ S_1^-}-\frac{1}{S_2^+ S_2^-}\right)(\sigma_3-\sigma_1)^2+\\
&\frac{1}{2}\left(\frac{1}{S_1^+ S_1^-}+\frac{1}{S_2^+ S_2^-}-\frac{1}{S_3^+ S_3^-}\right)(\sigma_1-\sigma_2)^2+\\
&\sum_{i=1}^{3}\left(\frac{1}{S_i^+}-\frac{1}{S_i^-}\right)\sigma_i+\sum_{i=4}^{6}\left(\frac{\sigma_i}{S_i}\right)^2 \geq 1
\end{aligned} \tag{5}$$

2.3.5 Hashin Criterion

The failure criteria discussed up to now only predict whether or not failure has occured; they make no attempt to diagnose the origin of the failure, i.e., whether it is in the fibres or the matrix. The Hashin criteria takes a step toward identifying the failure mode by proposing a series of conditional criteria, each tailored to a particular failure mechanism. By doing so, it introduces micro-mechanical knowledge into a macro-mechanical failure theory without introducing a lot of complexity. The Hashin criteria considers four separate failure modes: tensile and compressive failure of the fibres, and tensile and compressive failure of the matrix. Failure in the fibre modes occurs as a result of fibre breakage (in tension) or fibre buckling (in compression). The matrix modes both occur as a result of matrix cracking along a plane parallel with the fibres. The failure criteria are summarized as follows:

Tensile Fibre Mode, $\sigma_1 > 0$

$$\sigma_1/S_1^+ \geq 1 \tag{6}$$

Compressive Fibre Mode, $\sigma_1 < 0$

$$\sigma_1/S_1^- \geq 1 \tag{7}$$

Tensile Matrix Mode, $\sigma_2 + \sigma_3 > 0$

$$\frac{1}{S_2^+ S_3^+}(\sigma_2 + \sigma_3)^2 + \frac{1}{S_6^2}(\sigma_6^2 - \sigma_2\sigma_3) + \frac{1}{S_4 S_5}(\sigma_4^2 + \sigma_5^2) \geq 1 \tag{8}$$

Compressive Matrix Mode, $\sigma_2 + \sigma_3 < 0$

$$\frac{1}{\sqrt{S_2^- S_3^-}}\left[\frac{S_2^- S_3^-}{2S_6^2} - 1\right](\sigma_2 + \sigma_3) + \frac{1}{4S_6^2}(\sigma_2 + \sigma_3)^2 + \frac{1}{S_6^2}(\sigma_6^2 - \sigma_2\sigma_3) + \frac{1}{S_4 S_5}(\sigma_4^2 + \sigma_5^2) \geq 1 \tag{9}$$

The failure indices for the fibre and matrix modes are evaluated according to the signs of the normal stresses, as indicated above. The larger of the two failure indices is taken as the significant value for the purposes of first-ply failure.

2.3.6 Christensen Stress Criterion

In this criterion, separate polynomial failure equations are postulated for fibre- and matrix-related failures [16]. Coefficients of the polynomial expression are determined partly from measured strength data, and partly through micromechanical knowledge of and assumptions about the material behaviour. The resulting failure criteria are given as follows.

Matrix Mode

$$\alpha_1 k_1(\sigma_2 + \sigma_3) + (1 + 2\alpha_1)[\frac{1}{4}(\sigma_2 - \sigma_3)^2 + \sigma_{23}] + (\sigma_{12}^2 + \sigma_{13}^2) \geq k_1^2 \tag{10}$$

where

$$k_1 = S_{12} = |S_2^-|/2 \qquad \alpha_1 = \frac{1}{2}\left(\frac{|S_2^-|}{S_2^+} - 1\right)$$

Fibre Mode

$$-\alpha_2 k_2 \sigma_1 + \frac{1}{4}(1 + 2\alpha_2)\sigma_1^2 - \frac{(1 + \alpha_2)^2}{2}\sigma\sigma_1 \geq k_2^2 \tag{11}$$

where

$$\sigma = \frac{\sigma_2 + \sigma_3}{2} \qquad k_2 = S_1^+/2 \qquad \alpha_2 = \frac{1}{2}\left(\frac{S_1^+}{|S_1^-|} - 1\right)$$

3 Finite Element Methodology

3.1 Four-Node Composite Shell Element

A composite shell element "Shell4" was recently developed at DREA by the author for linear elastic analysis of laminates [24]. It is a four-node quadrilateral, and allows for symmetric and non-symmetric laminates with an arbitrary number of layers. Layers are allowed to have orthotropic or isotropic material properties, so that unidirectional, woven, and chopped strand type layers can be represented, as well as sandwich materials with laminate face sheets. The element stiffness formulation uses first-order shear deformation theory for the material model; it uses bilinear, isoparametric shape functions for displacements and rotations, with special corrective functions for transverse shear deformation, in-plane rotation and warping. A full description of the element formulation is given in Reference [24]. The Shell4 element has been implemented in a special-purpose finite element code "FELAM" for linear analysis of composite structures. This code is being used as the test vehicle for the first-ply failure analysis presented in this study.

3.2 Finite Element Stress and Strain Evaluation

The first-ply failure theories described in the previous section rely on accurate assessment of both laminar strengths and stresses. Strength assessment for composites is best obtained from experimental testing, and extensive data is available for the more common materials. It has already been observed that the laminar stresses being used are not the actual stresses in the material, but instead are approximations derived from smearing together the fibres and matrix into a homogeneous laminar material with anisotropic properties.

Finite element stresses and strains are evaluated on an element-by-element, layer-by-layer basis. Element strains are evaluated following the solution of the global displacements. The strain expressions are derived from the basic element displacement functions. The strain formula for Shell4 are quite complicated, as they involve separate expressions for membrane, bending and transverse shear that have to be combined together to obtain the total strain in a layer. More detailed information can be found in Reference [24]. The strain functions are typically evaluated in the element coordinate system xyz. Layer strains are then determined by evaluating the element strains at an elevation corresponding to the position of the layer, and then transforming the resulting strain to the laminate coordinate system 123.

The strain can be determined at any point within the layer of an element. Usually layers are thin enough that the strains will change little through the thickness of a layer, and it is sufficient to evaluate them at the layer middle surface. The position

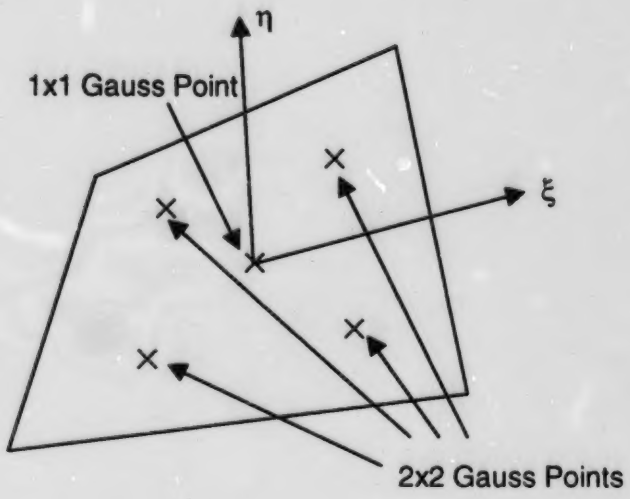

Figure 2: *Gauss point positions for the Shell4 element*

in the plane of the middle surface where the strains are evaluated depends on the type of element being used. If an element uses numerical integration at $n \times n$ Gauss points to formulate the stiffness matrix, the highest accuracy in the stresses and strains is obtained at the positions of the $n-1 \times n-1$ points. In the case of the Shell4 element, which is a bilinear, isoparametric type of element, 2×2 numerical integration is used. The strains are therefore evaluated at the 1×1 Gauss point, which is located at the origin of the natural coordinate system of the element (see Figure 2). Strains evaluated at a single point in a layer are effectively uniform across the element at that elevation.

Stresses are then evaluated from the strains using a stress-strain relationship that is of the following form for an orthotropic material:

$$\begin{Bmatrix} \sigma_1 \\ \sigma_2 \\ \sigma_3 \\ \sigma_4 \\ \sigma_5 \\ \sigma_6 \end{Bmatrix} = \begin{bmatrix} C_{11} & C_{12} & C_{13} & 0 & 0 & 0 \\ C_{12} & C_{22} & C_{23} & 0 & 0 & 0 \\ C_{31} & C_{32} & C_{33} & 0 & 0 & 0 \\ 0 & 0 & 0 & C_{44} & 0 & 0 \\ 0 & 0 & 0 & 0 & C_{55} & 0 \\ 0 & 0 & 0 & 0 & 0 & C_{66} \end{bmatrix} \begin{Bmatrix} \epsilon_1 \\ \epsilon_2 \\ \epsilon_3 \\ \epsilon_4 \\ \epsilon_5 \\ \epsilon_6 \end{Bmatrix} \tag{12}$$

The coefficients C_{ij} are laminar stiffnesses, which are functions of the fundamental laminar material properties. With this expression the stresses are obtained in the coordinate system of the layer. Appropriate tensor transformations can be applied to obtain stress quantities in the element, global, or some other coordinate system. In the case of thin layers, or even moderately thick layers, plane stress conditions

prevail so that $\sigma_3 = 0$ and the third row and column can be removed from (12).

3.3 First-Ply Failure Load and Location

The general approach to determining the first-ply failure load is to first perform a static analysis of the structure for the load distribution of interest. Failure indices are then determined using the failure criteria for all the layers of the elements in structure. The applied load is then scaled up or down, as required, until a maximum failure index of one is obtained. The resulting scaled load is the failure load.

Because failure theories are generally nonlinear functions of the stresses, the failure load is determined by an iterative process. Reddy and Pandey [23] have presented a finite-element based algorithm for evaluating first-ply failure loads. Their algorithm can be used in conjuction with non-linear FEA, so that the iterative process embraces both the solving of the displacements as well as scaling of the load. The present study adapts the Reddy and Pandey algorithm for use with linear FEA, resulting in a numerically more efficient algorithm. This additional efficiency comes from recognizing that in a linear analysis, scaling the load by a given factor produces stresses and strains that are scaled by the same factor. Thus, once an initial analysis has been performed to establish the initial stress/strain levels, the iterative procedure involves scaling the linear stresses or strains until a failure load condition is achieved. The procedure is illustrated in Figure 3.

With the failure theories considered in this study, the mode of failure is not explicitly identified except in the case of the Hashin and Christensen criteria. For the other theories, an estimate of the probable mode of failure can be obtained by examining the ratios of σ/S or ϵ/s at the failure location. If σ_1/S_1^+ is the largest (and if $\sigma_1 > 0$), a tensile failure in direction 1 is suggested; if σ_2/S_2^- is the largest (and if $\sigma_2 < 0$), a compressive failure in direction 2 is suggested; and so on. Direction 1 failures may be interpreted as fibre breakage or buckling, whereas direction 2 failures may be interpreted as matrix cracking. Failures in a shear component may also be interpreted as matrix failures. Although this simple method ignores coupled mechanisms and more sophisticated failures such as delaminations and fibre pull-out, it may provide the analyst with a clue as to failure origin.

3.4 Implementation

The first-ply failure analysis method illustrated in Figure 3 has been implemented in the finite element programme FELAM. This is a special purpose FEA code for composite plate and shell structure which has been under development at DREA since 1999. The programme uses an object-oriented design coded in C++, the basic arrangement of which is illustrated in Figure 4. The programme uses two principal

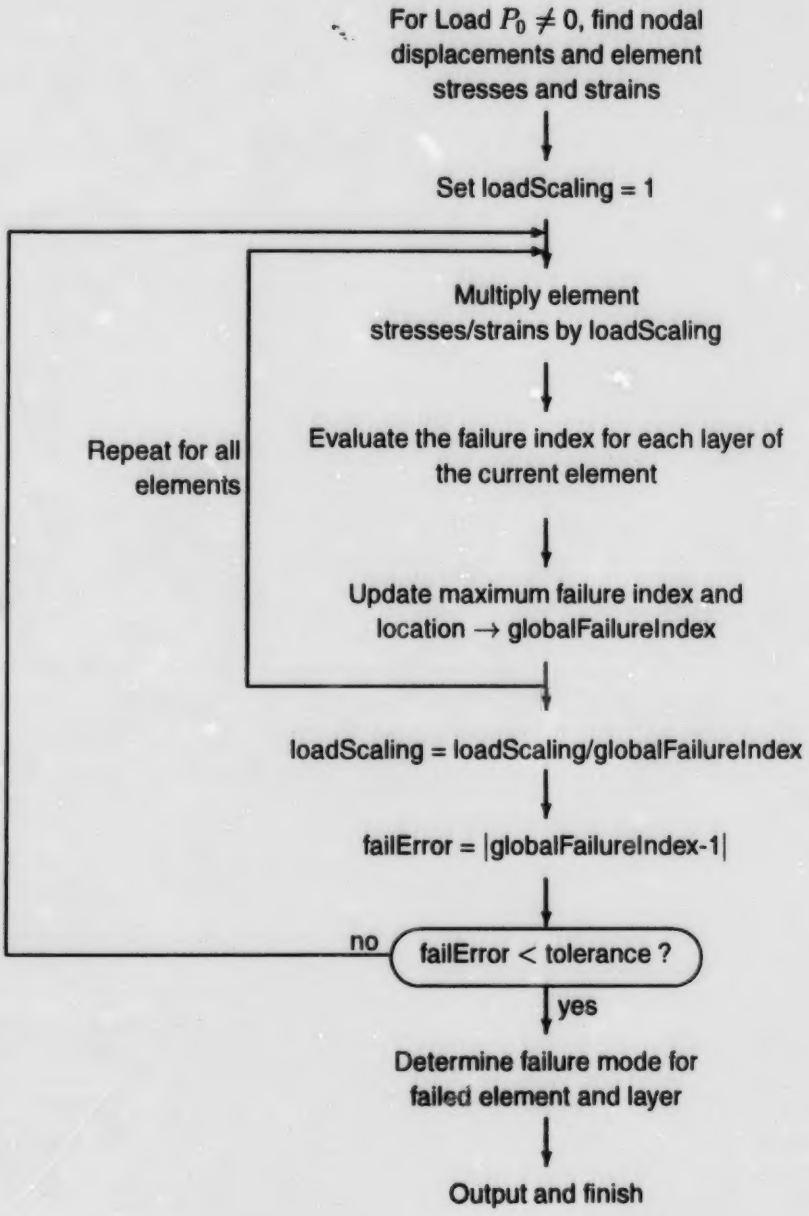
For Load $P_0 \neq 0$, find nodal displacements and element stresses and strains
Set loadScaling = 1
Multiply element stresses/strains by loadScaling
Evaluate the failure index for each layer of the current element
Repeat for all elements
Update maximum failure index and location → globalFailureIndex
loadScaling = loadScaling/globalFailureIndex
failError = |globalFailureIndex-1|
no
failError < tolerance ?
yes
Determine failure mode for failed element and layer
Output and finish

***Figure 3:** Algorithm for Determining First-Ply Failure Load*

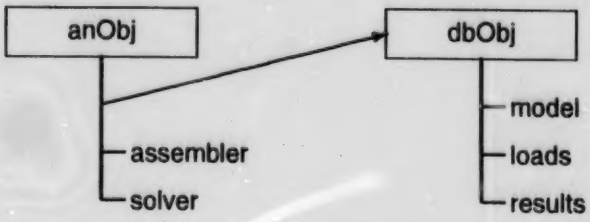

***Figure 4:** Architecture of the Felam Program*

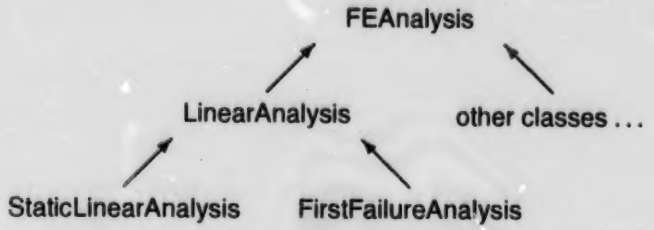

***Figure 5:** Hierarchy of FELAM Analysis Classes*

objects: a finite element database object dBObj, and an analysis object anObj. The database object reads and stores all the data defining the finite element model, loads and results. This data is held in several container objects, each of which holds and manages objects belonging to general class types, such as nodes, elements, materials, loads, displacements and stresses.

The analysis object is created at run time, according to the type of analysis requested by the user. A pointer to the database object is passed to the analysis object, which then assembles and solves the global equations. The global solution is passed to the database object for post-computation of stresses and output.

A first-ply failure analysis is carried out by creating the analysis object of a derived class type FirstFailureAnalysis. An object of this class contains all the methods required to execute the procedure in Figure 3. The hierarchy of derived analysis classes is shown in Figure 5. At the present stage of the programme development, analysis objects can only be created from the StaticLinearAnalysis and and FirstFailureAnalysis classes.

Failure criteria have been implemented as objects from a hierarchy of derived classes shown in Figure 6. Note that some additional failure criteria have been included for

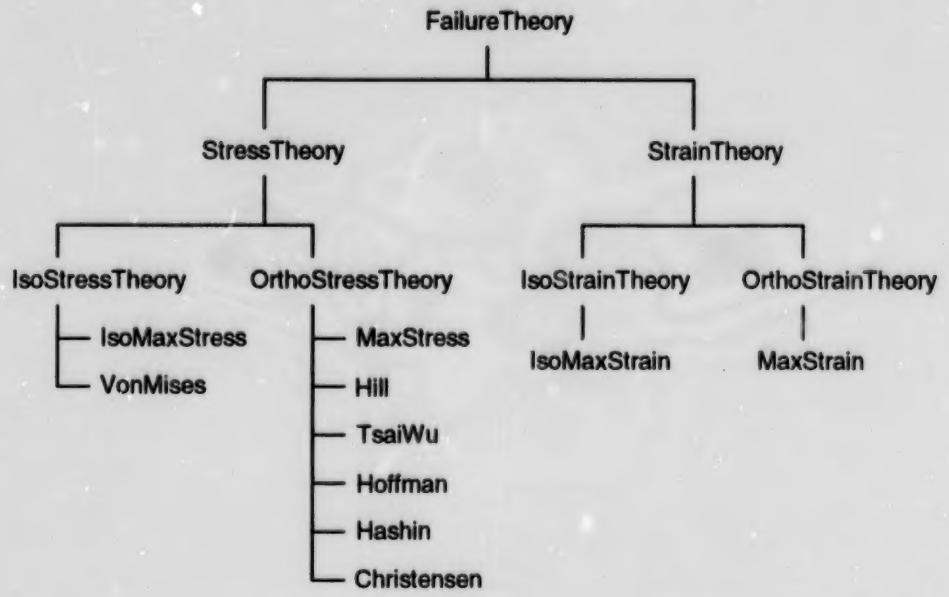

***Figure 6:** Hierarchy of Failure Classes*

isotropic materials. The first-ply failure method, when it is applied to elements with isotropic material properties, is equivalent to the first-yield method. Though this application is not considered in the present study, it has been included in FELAM.

Failure objects are contained as data in objects created from the material classes (Figure 7). Orthotropic material objects can only contain failure objects derived from either OrthoStressTheory or OrthoStrainTheory. The failure theory objects are responsible for storing the essential data defining the failure theory (i.e., the coefficients of the failure criterion), and for returning a failure index for a given stress or strain state.

An example of a FELAM input file is given in Annex A. It contains the definition model along with its laminated material properties and associated failure criterion.

4 Numerical Results

In this section the first-ply failure algorithm is demonstrated on a 9×5 inch simply-supported plate model, shown in Figure 8. A similar model was used by Reddy and Pandey [23]. The model is tested for the nine different lamination schemes listed in Table 1, for both uniform normal and in-plane loading. Following this, a circular hole is introduced in the plate and the analyses are repeated in order to

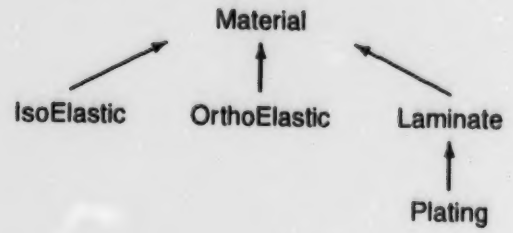

***Figure 7:** Hierarchy of Material Classes*

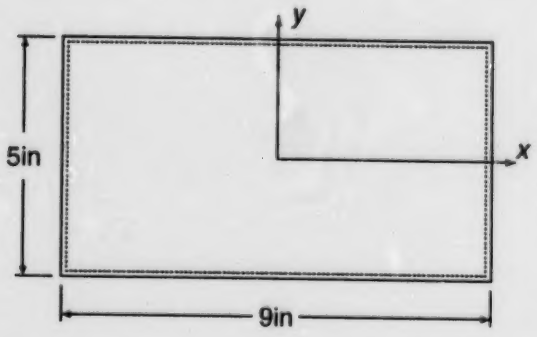

***Figure 8:** 9× 5in Simply-Supported Plate Model*

assess the stress concentration effect. The ply thickness is 0.005 in for all cases. Two different material properties are considered: unidirectional plies of T300/5208 graphite epoxy (Table 2) and unidirectional plies of a glass-fibre, polyester resin (fibreglass, see Table 3). Of the two, graphite epoxy is stronger in compression in the fibre direction, but weaker in compression normal to the fibres. It is also substantially stiffer than the fibreglass in the fibre direction.

One-quarter models are used where permitted by symmetry or antisymmetry in the lamination scheme. Figures 9 and 10 show boundary conditions applied to the one-quarter models for symmetric and antisymmetric lamination schemes, respectively. In these figures u, v, and w denote displacement variables in the x, y, and z directions, respectively (see Figure 8), whereas ψ_x and ψ_y denote rotations about the x and y directions. Cross-ply laminates F, G, and H use the symmetric configuration; angle-ply laminate I uses the antisymmetry configuration. All other laminate schemes use the full plate model.

Table 1: *Nine lamination schemes used in the plate model analysis [23].*

Name	No. of Layers	Lamination Scheme†
A	3	[45/-45/45]
B	16	$[45/-45/90/0/45/90/-45/0]_S$
C	16	$[45/-45/0/90/45/0/-45/90]_S$
D	16	$[45/0/-45/0/-45/90/0/45]_S$
E	16	$[45/0/-45/0/-45/0/45/0]_S$
F	4	$[0/90]_S$
G	2	[0/90]
H	4	[0/90/0/90]
I	4	[45/-45/45/-45]

†Ply sequences are denoted as $[\theta_1/\theta_2/\ldots]$, where θ_i is the ply angle of the i^{th} layer. The subscript S indicates that the ply sequence is symmetric, and so only half of the ply angles are given.

Table 2: *Material properties for T300/5208 graphite epoxy.*

Properties	Values
E_1	19,200 ksi
E_2	1560 ksi
E_3	1560 ksi
$G_{12} = G_{13}$	820 ksi
G_{13}	490 ksi
$\nu_{12} = \nu_{13}$	0.24
ν_{23}	0.49
S_1^+	219.5 ksi
S_1^-	–246.0 ksi
$S_2^+ = S_3^+$	6.35 ksi
$S_2^- = S_3^-$	–6.35 ksi
$S_{12} = S_{13}$	12.6 ksi
S_{23}	9.80 ksi
Ply thickness	0.005 in

Table 3: *Material Properties for Fibreglass.*

Properties	Values
E_1	6740 ksi
$E_2 = E_3$	1010 ksi
$G_{12} = G_{13}$	1010 ksi
G_{13}	510 ksi
$\nu_{12} = \nu_{13}$	0.25
S_1^+	231.7 ksi
S_1^-	–72.4 ksi
$S_2^+ = S_3^+$	5.79 ksi
$S_2^- = S_3^-$	–29.0 ksi
$S_{12} = S_{13}$	8.69 ksi
S_{23}	4.35 ksi
Ply thickness	0.005 in

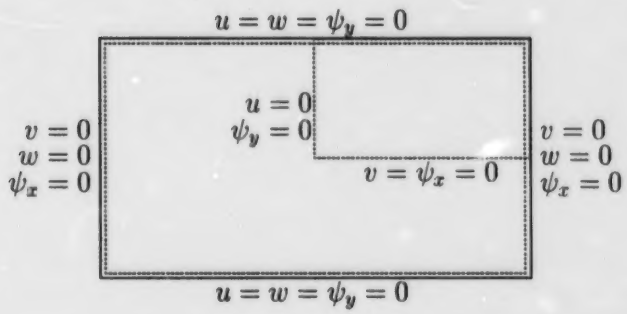

Figure 9: *Symmetric Quarter-Plate Model Used for Cross-Ply Laminates.*

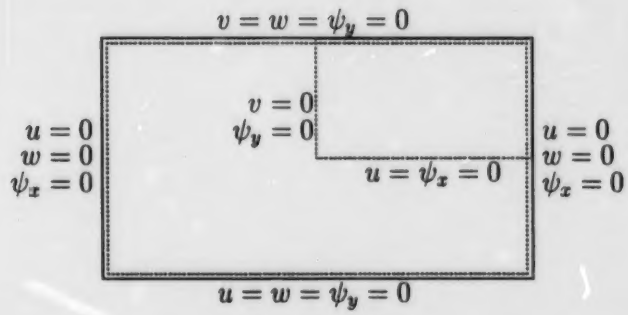

Figure 10: *Anti-Symmetric Quarter-Plate Model Used for Angle-Ply Laminates.*

***Table 4:** Analytical and FE Maximum Deflections for Uniform Pressure Loading of a 9x5 Plate Model.*

Lamination Scheme	Laminate Type	Pressure Load	Exact [23] (in)	FE Solutions (in) 2×2	4×4	8×8
[0/90]	cross-ply	0.1	1.884	1.842	1.873	1.882
[0/90/0/90]	cross-ply	0.1	0.135	0.132	0.134	0.135
[0/90/90/0]	cross-ply	0.1	0.230	0.221	0.228	0.229
[45/-45/45/-45]	angle-ply	0.1	0.109	0.107	0.108	0.109

4.1 Normal Loading

4.1.1 Displacement Validation

A uniformly distributed normal pressure load is applied to the plate models. Analytical solutions from Classical Laminate Theory are available for cross-ply and angle-ply laminates. They are valid for thin laminates with a span to total-thickness ratio $(a/h) > 100$. In Table 4, comparisons between the analytical and FE results are given for the maximum plate deflection for graphite epoxy. Three levels of FE mesh refinement were used with the quarter-plate to obtain these results. It was determined here and in a previous study [24] that 8×8 refinement produces sufficiently accurate displacements and stresses in the quarter-plate models (i.e., 16×16 in the full plate models).

4.1.2 Failure Loads and Locations

Uniform pressure failure loads were predicted for the 9×5 plate structure using the nine laminate schemes and six stress-based failure theories. The results of the failure predictions are given for both materials in Tables 5–13. In addition to the failure load magnitude, the location of failure is identified (by element and layer number), as is the probable direction (mode) of failure. For reference, the element numbering scheme used in the symmetric and full-plate models is given in Figures 11 and 12, respectively.

Good consistency is achieved in the predicted failure loads for graphite epoxy, the exception being the Christensen criterion which predicts substantially lower failure loads for all laminates except G and H. For fibreglass, good consistency is obtained for all except the Tsai-Hill criterion, which underpredicts by fifty percent or more failure of laminates A–E, and I, and somewhat overpredicts failure of the cross-ply laminates F–H.

The poor results for the Christensen criterion with Gr-Ep has to do with an incon-

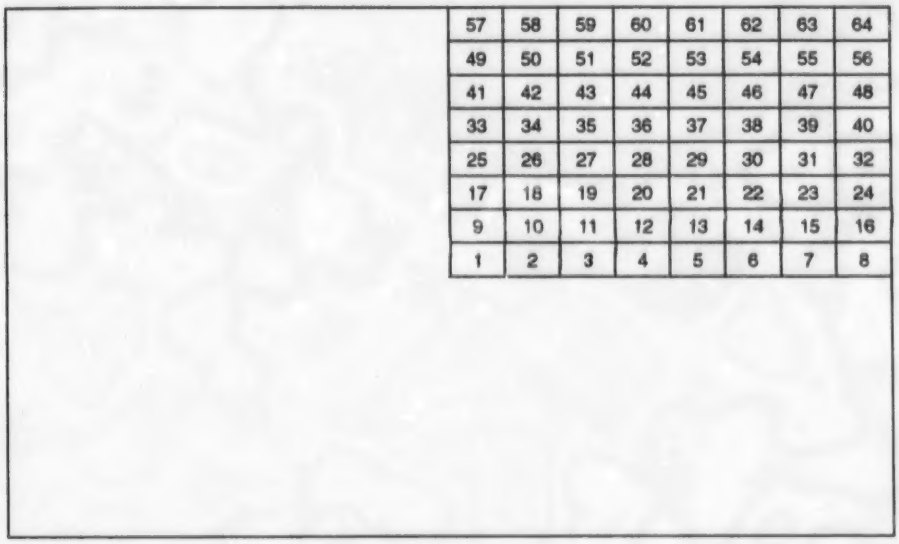

***Figure 11:** Element Numbering Scheme for Symmetric Plate Models.*

241	242	243	244	245	246	247	248	249	250	251	252	253	254	255	256
225	226	227	228	229	230	231	232	233	234	235	236	237	238	239	240
209	210	211	212	213	214	215	216	217	218	219	220	221	222	223	224
193	194	195	196	197	198	199	200	201	202	203	204	205	206	207	208
177	178	179	180	181	182	183	184	185	186	187	188	189	190	191	192
161	162	163	164	165	166	167	168	169	170	171	172	173	174	175	176
145	146	147	148	149	150	151	152	153	154	155	156	157	158	159	160
129	130	131	132	133	134	135	136	137	138	139	140	141	142	143	144
113	114	115	116	117	118	119	120	121	122	123	124	125	126	127	128
97	98	99	100	101	102	103	104	105	106	107	108	109	110	111	112
81	82	83	84	85	86	87	88	89	90	91	92	93	94	95	96
65	66	67	68	69	70	71	72	73	74	75	76	77	78	79	80
49	50	51	52	53	54	55	56	57	58	59	60	61	62	63	64
33	34	35	36	37	38	39	40	41	42	43	44	45	46	47	48
17	18	19	20	21	22	23	24	25	26	27	28	29	30	31	32
1	2	3	4	5	6	7	8	9	10	11	12	13	14	15	16

***Figure 12:** Element Numbering Scheme for Full Plate Models.*

sistency in the assumptions in the theory and the actual properties of the material. Eq. (10) indicates that $S_{12} = |S_2^-|/2$ is assumed for the material, whereas the properties in Table 2 suggest $S_{12} \approx 2|S_2^-|$. For comparison, the fibreglass properties of Table 3 give $S_{12} \approx |S_2^-|/3$, which is closer to the Christensen assumption. The poor results with the Tsai-Hill criterion for fibreglass is indicative of the absence of first-order terms in its polynomial expression. First-order terms allow the centre of the failure ellipse to be shifted away from the origin of the stress plane, as is required when materials have differing compressive and tensile strengths. In Gr-Ep, where the tensile and compressive properties are similar, errors due to a centred failure envelope are not noticeable. But this is clearly not the case with the fibreglass.

Overall, the load carrying capacity of the fibreglass laminates is less than the corresponding graphite epoxy laminates, as would be expected. The cross-ply laminates F–H are more closely matched in terms of their load carrying capacities than the other laminates.

Reddy and Pandey reported failure loads for the same model, using four of the same failure theories, and using a similar T300 graphite epoxy material. Their results are compared with FELAM results in Table 14, where it can be seen that the correlation in the predicted failure loads is generally poor. (The results compared used similar element types, with similar levels of mesh refinement.) Excellent agreement was only obtained for laminate F using the Maximum Stress, Hoffman, and Tsai-Wu criteria. Acceptable agreement was obtained for the same three criteria in laminates D and E. Very poor correlation was obtained with the Tsai-Hill criterion for all the laminates. In fact, Reddy and Pandey report failure loads for the Tsai-Hill criterion that were very much lower than the other criteria, similar to what was found with the fibreglass results presented here. However these Gr-Ep results could not be reproduced here.

To investigate this further, additional comparisons were performed using the commercial finite element programme ANSYS. ANSYS is able to calculate failure indices using three criteria (Maximum Stress, Maximum Strain, and Tsai-Wu) for either of its two composite shell elements (SHELL91 and SHELL99). It is unable to calculate the failure load directly by means of an algorithm such as the one in Figure 3. Instead, the failure loads have to be determined indirectly from the failure indices. Table 15 gives the failure indices, loads and locations predicted by ANSYS for Gr-Ep using its Maximum Stress criterion. In the table, these are compared with the corresponding FELAM results. Good agreement is obtained in all except the two angle ply laminates (A and I).

Table 5: *First-Ply Failure for Uniform Pressure Loading of Laminate A.*

Failure Criteria	T300				Fiberglass			
	Load (psi)	Elem.	Layer	Mode	Load (psi)	Elem.	Layer	Mode
Max. Stress	1.019	121	1, 3	+2, -2	0.558	241	3	-1
Hoffman	0.898	241	1	+1	0.380	241	3	-1
Tsai-Wu	0.749	241	1	+1	0.361	241	3	-1
Tsai-Hill	0.905	241	1	+1	0.187	241	3	-1
Hashin	0.945	121	3	-2	0.511	136	1	+2
Christensen	0.668	121	1, 3	+2, -2	0.549	241	3	-1

Table 6: *First-Ply Failure for Uniform Pressure Loading of Laminate B.*

Failure Criteria	T300				Fiberglass			
	Load (psi)	Elem.	Layer	Mode	Load (psi)	Elem.	Layer	Mode
Max. Stress	25.16	120	1,16	+2, -2	14.24	120	1	+2
Hoffman	23.91	137	1	+2	12.77	16	16	+2
Tsai-Wu	25.77	16	15	-2	12.09	16	16	+2
Tsai-Hill	23.44	120	1	+2	6.113	16	16	+2
Hashin	23.73	120	16	-2	11.91	137	1	+2
Christensen	15.36	241	3,14	12	12.75	120	1	+2

Table 7: *First-Ply Failure for Uniform Pressure Loading of Laminate C.*

Failure Criteria	T300				Fiberglass			
	Load (psi)	Elem.	Layer	Mode	Load (psi)	Elem.	Layer	Mode
Max. Stress	20.08	121	3,14	+2, -2	12.90	136	3	+2
Hoffman	21.31	137	1	+2	11.88	120	1	+2
Tsai-Wu	22.89	136	3	+2	11.30	241	16	+2
Tsai-Hill	20.93	136	3	+2	5.718	241	16	+2
Hashin	21.23	136	16	-2	10.95	120	1	+2
Christensen	14.08	16	3,14	12	11.69	120	1	+2

Table 8: *First-Ply Failure for Uniform Pressure Loading of Laminate D.*

Failure Criteria	T300				Fiberglass			
	Load (psi)	Elem.	Layer	Mode	Load (psi)	Elem.	Layer	Mode
Max. Stress	15.66	121	2,15	+1	9.584	136	2	+2
Hoffman	15.33	136	2	+1	10.40	241	2	12
Tsai-Wu	16.27	136	2	+1	10.40	241	2	12
Tsai-Hill	15.61	121	2	+1	5.285	241	16	+2
Hashin	15.66	121	15	-2	9.582	136	2	+2
Christensen	10.70	16	2,15	12	9.583	136	2	+2

Table 9: *First-Ply Failure for Uniform Pressure Loading of Laminate E.*

Failure Criteria	T300				Fiberglass			
	Load (psi)	Elem.	Layer	Mode	Load (psi)	Elem.	Layer	Mode
Max. Stress	15.05	121	2,15	+1	9.2874	121	2	+2
Hoffman	14.93	136	2	+1	9.9795	241	2	12
Tsai-Wu	15.64	136	2	+1	9.9806	241	2	12
Tsai-Hill	15.00	121	2	+1	5.0976	241	16	+2
Hashin	15.05	121	15	-2	9.2855	121	2	+2
Christensen	10.14	241	2,15	12	9.2863	121	2	+2

Table 10: *First-Ply Failure for Uniform Pressure Loading of Laminate F.*

Failure Criteria	T300				Fiberglass			
	Load (psi)	Elem.	Layer	Mode	Load (psi)	Elem.	Layer	Mode
Max. Stress	0.586	1	1,4	+2, -2	0.465	1	1	+2
Hoffman	0.707	1	1	+2	0.509	1	1	+2
Tsai-Wu	0.744	1	1	+2	0.528	1	1	+2
Tsai-Hill	0.710	1	1	+2	0.572	64	4	12
Hashin	0.711	1	4	-2	0.465	1	1	+2
Christensen	0.469	64	1, 4	12	0.465	1	1	+2

Table 11: *First-Ply Failure for Uniform Pressure Loading of Laminate G.*

Failure Criteria	T300				Fiberglass			
	Load (psi)	Elem.	Layer	Mode	Load (psi)	Elem.	Layer	Mode
Max. Stress	0.122	1	1	+2	0.110	1	1	+2
Hoffman	0.122	1	1	+2	0.112	1	1	+2
Tsai-Wu	0.122	1	1	+2	0.113	1	1	+2
Tsai-Hill	0.122	1	1	+2	0.135	1	1	+2
Hashin	0.122	1	4	+2	0.110	1	1	+2
Christensen	0.122	1	1	+2	0.110	1	1	+2

Table 12: *First-Ply Failure for Uniform Pressure Loading of Laminate H.*

Failure Criteria	T300				Fiberglass			
	Load (psi)	Elem.	Layer	Mode	Load (psi)	Elem.	Layer	Mode
Max. Stress	0.796	1	1	+2	0.542	1	1	+2
Hoffman	0.793	1	1	+2	0.570	1	1	+2
Tsai-Wu	0.812	1	1	+2	0.581	1	1	+2
Tsai-Hill	0.795	1	1	+2	0.760	64	6	12
Hashin	0.796	1	1	+2	0.542	1	1	+2
Christensen	0.727	1	1	+2	0.542	1	1	+2

Table 13: *First-Ply Failure for Uniform Pressure Loading of Laminate I.*

Failure Criteria	T300				Fiberglass			
	Load (psi)	Elem.	Layer	Mode	Load (psi)	Elem.	Layer	Mode
Max. Stress	2.103	1	1	+2	1.175	1	1	+2
Hoffman	1.828	1	1	+2	1.035	1	1	+2
Tsai-Wu	2.221	1	1	+2	1.034	64	1	-1
Tsai-Hill	1.853	1	1	+2	0.525	64	1	-1
Hashin	1.866	1	4	-2	0.937	1	1	+2
Christensen	1.329	1	1	+2	1.020	1	1	+2

Table 14: *Correlation of Failure Load Results with Reddy and Pandey[23].*

Failure Criteria	Laminate Scheme A	B	C	D	E	F	G	H	I
Max. Stress	3.27†	1.22	1.10	1.10	1.12	0.999	0.316	0.388	1.42
Hoffman	3.06	1.28	1.29	1.10	1.12	1.005	0.318	0.442	1.38
Tsai-Wu	2.37	1.26	1.27	1.11	1.13	1.015	0.311	0.394	1.60
Tsai-Hill	7.64	3.36	3.39	2.90	2.96	1.84	0.593	1.30	3.06

†Values are given as ratios of predicted FELAM failure loads to Reddy and Pandey's failure loads.

Table 15: *First-Ply Failure Predicted by ANSYS and FELAM for the Maximum Stress Criterion.*

Laminate Scheme	ANSYS Mesh	ANSYS Failure Load (psi)	FELAM Mesh	FELAM Failure Load (psi)	% Diff.
A	8×8	0.730	16×16	1.019	-27.8
B	8×8	24.34	16×16	25.16	-3.2
C	8×8	21.58	16×16	20.08	7.5
D	8×8	15.59	16×16	15.66	-0.4
E	8×8	14.99	16×16	15.05	-0.4
F	4×4	0.582	8×8	0.586	-0.7
G	4×4	0.121	8×8	0.122	-0.8
H	4×4	0.796	8×8	0.796	0
I	4×4	1.633	8×8	2.103	-22.3

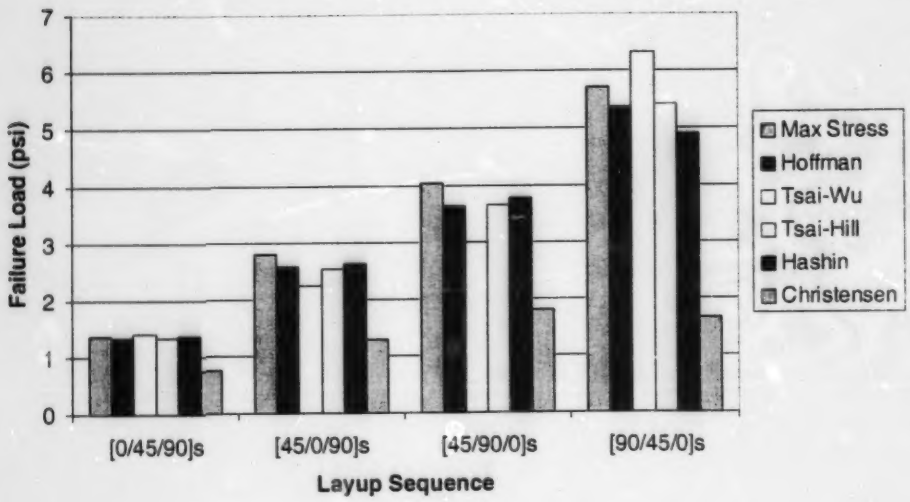

Figure 13: *Effect of Lay-Up Sequence on First-Ply Normal Failure Load of Gr-Ep Laminates.*

4.1.3 Effect of Layer Sequence

The effect of four different layer sequences in a symmetric laminate was examined for the same example plate problem. The results given in Figures 13 and 14 and confirm what is intuitively expected: that highest failure loads are obtained with the 90 degree layers (i.e., layers with the fibres in the direction of the shorter dimension of the plate) positioned on the outside of the laminate. In this arrangement the highest strains in the plate are aligned with the fibres.

4.2 In-Plane Loading

The 9×5 plate problem also was analysed with a uniaxial uniform load along the short side, as shown in Figure 15. A one inch diameter circular hole was introduced at the centre of the plate in order to create a stress concentration. A finite element mesh with considerable refinement in the vicinity of the hole was used as shown in Figure 16. A full-plate model was used for laminates A–E, and I; a quarter-plate model of the same mesh was used for laminates F, G, and H. The results are given in Tables 16–24, in which the failure loads are forces per unit length applied uniformly along the loaded edge. The tables give the layer numbers where failure occurs and the locations for failure of Gr-Ep are shown in Figure 16. The same location was predicted for all of the theories with every laminate except for schemes A and E, as indicated in the figure.

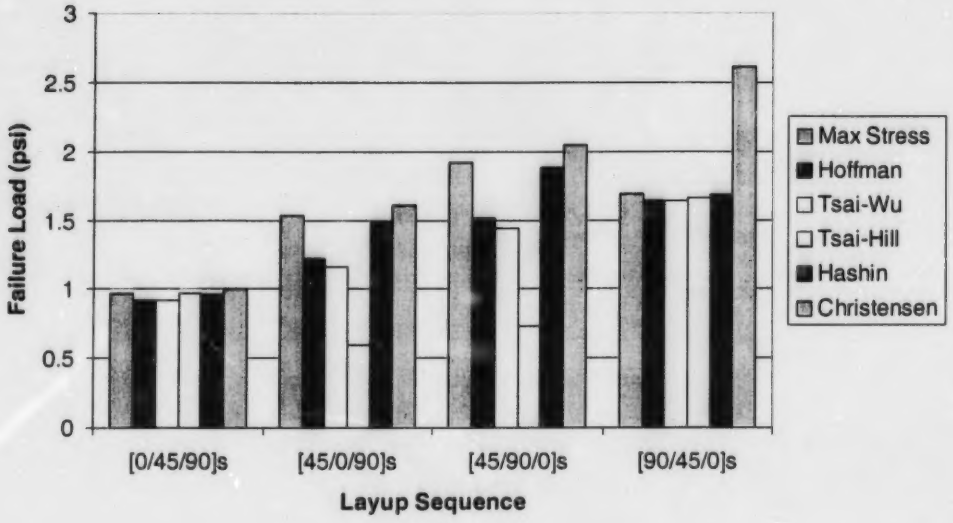

Figure 14: *Effect of Lay-Up Sequence on First-Ply Normal Failure Load with Fibreglass Laminates.*

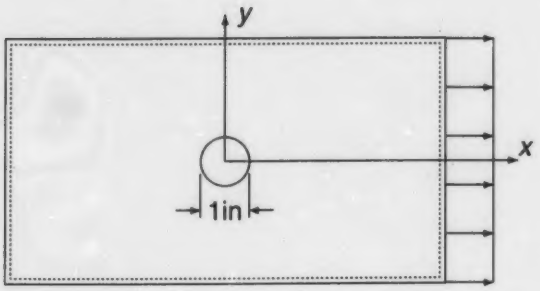

Figure 15: *9x5 Plate Model with Hole and In-Plane Uniaxial Loading*

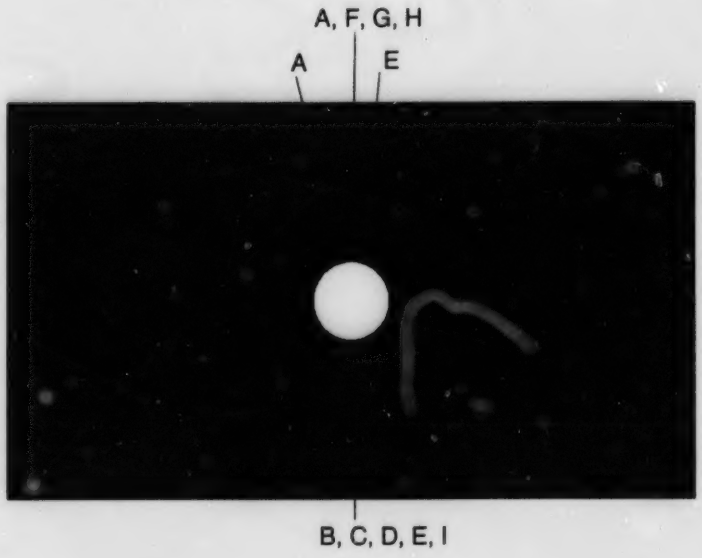

***Figure 16:** Mesh for 9x5 Plate Models with Circular Hole (All Laminates). Failure Locations Predicted for the Nine Laminates Are Shown.*

All of the analyses predict failure locations in elements on the perimeter of the hole, close to where the perimeter is intersected by the y-axis. This is where stress concentrations are known to occur for similar geometries with isotropic materials. Validation of the failure loads was achieved by comparison with ANSYS results for a similar finite element mesh. The maximum stress criterion was used to obtain the ANSYS failure loads, which are found to be one to ten percent lower than their FELAM counterparts (Table 25). This can be partly accounted for by the fact that ANSYS stresses are somewhat higher than FELAM stresses because ANSYS predicts stresses at nodes and not at integration points inside the element, as FELAM does. In this case, the ANSYS nodal stresses are closer to the stress concentration, and are therefore somewhat higher than the corresponding FELAM stresses. The mesh has been sufficiently refined that the differences between nodal and element stresses are not significant enough to affect the character of the results, although minor differences in the failure loads may be observed.

Generally, good consistency is observed among four of the six failure criterion. As with the normal loading results, the Christensen and Tsai-Hill criteria proved to be unreliable, for the same reasons described in the discussion of the normal loading results. Additional discrepancies appeared in the angle-ply laminates A and I, where the Maximum Stress criterion over-predicts the load at which failure occurs in the shear mode; and in laminates B, C and D, where the Tsai-Wu criteria under-predicts the failure load. Both of these behaviours are observable in laminate

***Table 16:** First-Ply Failure for In-Plane Loading of Laminate A with Hole.*

Failure	T300 Graphite Epoxy			Fibreglass		
Criteria	Load (lb/in)	Layer	Mode	Load (lb/in)	Layer	Mode
Max. Stress	169.92	1,2,3	12	94.91	1,2,3	12
Hoffman	150.03	2	12	77.45	2	12
Tsai-Wu	151.72	2	12	78.11	2	12
Tsai-Hill	150.36	2	12	137.09	1	+2
Hashin	150.43	2	12	82.34	2	12
Christensen	42.55	2	12	100.42	2	12

E as well.

To investigate the sensitivity of the various laminates to the stress concentration, the same analyses were repeated for in-plane loading of the plate without the hole. For these analyses a 16×16 mesh was used (8×8 for quarter-plate models). Figure 17 shows the ratios of the predicted failure loads with and without the hole for all of the cases examined. (Laminate C produces results identical to laminate B.) What is immediately noticeable is that the laminate G appears to be less affected by the presence of the hole than the others. This is due to the large contribution of out-of-plane bending that occurs with laminate G due to its lack of symmetry and relative thinness. (The maximum out-of-plane deflection for this laminate is about two orders of magnitude larger than the maximum in-plane displacement.) Although introducing the hole does reduce the failure load by about 20 percent, the laminate without the hole is already severely weakened due to bending-induced stresses. The results for unsymmetric laminates H and I are also affected by a bending component, though it is not as severe as for laminate G. Among symmetric laminates, the angle-ply laminate A appears to be the least affected by the presence of the hole.

An additional comparison of the in-plane loading results is provided in Figure 18 which shows the failure load per layer. This effectively indicates the relative strength of each laminate for loads in the x direction. Laminate E is by far the strongest, by virtue of having a high percentage of 0° layers and no 90° layers. Clearly the strongest laminate would have all 0° layers, but it would have little practical use as it be unable to support a significant load in any other direction.

4.3 Angle-Ply Laminates

The behaviour of anti-symmetric two-layer angle-ply laminates $[\theta/-\theta]$ and four-layer angle-ply laminates $[\theta/-\theta/\theta/-\theta]$ are now examined as a function of the ply

Table 17: *First-Ply Failure for In-Plane Loading of Laminate B with Hole.*

Failure Criteria	T300 Graphite Epoxy			Fibreglass		
	Load (lb/in)	Layer	Mode	Load (lb/in)	Layer	Mode
Max. Stress	879.73	3,6,11,14	+2	533.64	3,6,11,14	+2
Hoffman	879.22	3,6,11,14	+2	509.40	3,6,11	+2
Tsai-Wu	841.98	3	+2	503.07	3,6,11,14	+2
Tsai-Hill	875.09	3	+2	387.19	14	+2
Hashin	879.49	3	+2	532.92	3,6,11,14	12
Christensen	577.6	2,7,10,15	+2	533.21	3,6,11,14	+2

Table 18: *First-Ply Failure for In-Plane Loading of Laminate C with Hole.*

Failure Criteria	T300 Graphite Epoxy			Fibreglass		
	Load (lb/in)	Layer	Mode	Load (lb/in)	Layer	Mode
Max. Stress	879.73	4,8,9	+2	533.64	4,8,9,13	+2
Hoffman	879.22	4,8,9,13	+2	509.40	4	+2
Tsai-Wu	841.98	4,8,9	+2	503.07	8,9	+2
Tsai-Hill	875.09	4,8,9	+2	387.19	8,9,13	+2
Hashin	879.49	4,8,9	+2	532.92	4,8,9,13	+2
Christensen	577.6	2	+2	533.21	4,8,9,13	+2

Table 19: *First-Ply Failure for In-Plane Loading of Laminate D with Hole.*

Failure Criteria	T300 Graphite Epoxy			Fibreglass		
	Load (lb/in)	Layer	Mode	Load (lb/in)	Layer	Mode
Max. Stress	1058.2	6,11	+2	614.35	6,11	+2
Hoffman	1054.8	6,11	+2	571.19	3,5,12,14	12
Tsai-Wu	994.25	6,11	+2	568.82	6,11	+2
Tsai-Hill	1048.2	6,11	+2	416.20	6,11	+2
Hashin	1057.8	6,11	+2	601.89	3,5,12,14	12
Christensen	642.64	3,5,12,14	+2	613.65	6,11	+2

Table 20: *First-Ply Failure for In-Plane Loading of Laminate E with Hole.*

Failure Criteria	T300 Graphite Epoxy			Fibreglass		
	Load (lb/in)	Layer	Mode	Load (lb/in)	Layer	Mode
Max. Stress	1714.2	7,10,16	+2	762.97	1,3,5,7,10 12,14,16	12
Hoffman	1630.5	1,7,10,16	+2	613.19	3,5,12,14	12
Tsai-Wu	1571.5	16	+2	618.52	3,5,12,14	12
Tsai-Hill	1624.2	1,7,10,16	+2	742.17	16	2
Hashin	1629.6	1,7,10,16	+2	653.94	3,5,12,14	12
Christensen	632.36	3,5,12,14	12	775.90	12,14	12

Table 21: *First-Ply Failure for In-Plane Loading of Laminate F with Hole.*

Failure Criteria	T300 Graphite Epoxy			Fibreglass		
	Load (lb/in)	Layer	Mode	Load (lb/in)	Layer	Mode
Max. Stress	200.57	2,3	+2	135.40	2,3	+2
Hoffman	199.81	2,3	+2	133.62	2,3	+2
Tsai-Wu	210.09	2,3	+2	133.78	2,3	+2
Tsai-Hill	199.96	2,3	+2	132.96	2,3	+2
Hashin	199.94	2,3	+2	135.00	2,3	+2
Christensen	101.24	2,3	+2	135.16	2,3	+2

Table 22: *First-Ply Failure for In-Plane Loading of Laminate G with Hole.*

Failure Criteria	T300 Graphite Epoxy			Fibreglass		
	Load (lb/in)	Layer	Mode	Load (lb/in)	Layer	Mode
Max. Stress	102.03	2	+2	68.34	2	+2
Hoffman	101.66	2	+2	67.73	2	+2
Tsai-Wu	102.46	2	+2	67.90	2	+2
Tsai-Hill	101.76	2	+2	70.51	2	+2
Hashin	101.75	2	+2	68.15	2	+2
Christensen	52.72	2	+2	68.23	2	+2

Table 23: *First-Ply Failure for In-Plane Loading of Laminate H with Hole.*

Failure Criteria	T300 Graphite Epoxy			Fibreglass		
	Load (lb/in)	Layer	Mode	Load (lb/in)	Layer	Mode
Max. Stress	200.6	4	+2	135.23	4	+2
Hoffman	199.98	4	+2	132.84	2	+2
Tsai-Wu	201.56	2	+2	132.88	2	+2
Tsai-Hill	200.17	4	+2	128.06	2	+2
Hashin	200.15	4	+2	134.92	4	+2
Christensen	97.44	1	12	135.04	4	+2

Table 24: *First-Ply Failure for In-Plane Loading of Laminate I with Hole.*

Failure Criteria	T300 Graphite Epoxy			Fibreglass		
	Load (lb/in)	Layer	Mode	Load (lb/in)	Layer	Mode
Max. Stress	230.71	4	12	129.37	4	12
Hoffman	208.69	3	12	108.09	2	12
Tsai-Wu	211.77	3	12	109.03	2	12
Tsai-Hill	209.39	3	12	211.30	3	12
Hashin	209.75	3	12	114.12	3	12
Christensen	57.63	3	12	142.35	2	12

Table 25: *First-Ply Failure Predicted by ANSYS and FELAM for the Maximum Stress Criterion.*

Laminate Scheme	ANSYS Failure Load (lb/in)	FELAM Failure Load (lb/in)	% Diff.
A	168.13	169.92	-1.65
B	855.43	879.73	-2.76
C	855.43	879.73	-2.76
D	1024.8	1058.2	-3.16
E	1595.2	1714.2	-6.94
F	181.59	200.57	-9.46
G	91.89	102.03	-9.94
H	182.05	200.6	-9.25
I	227.14	230.71	-1.55

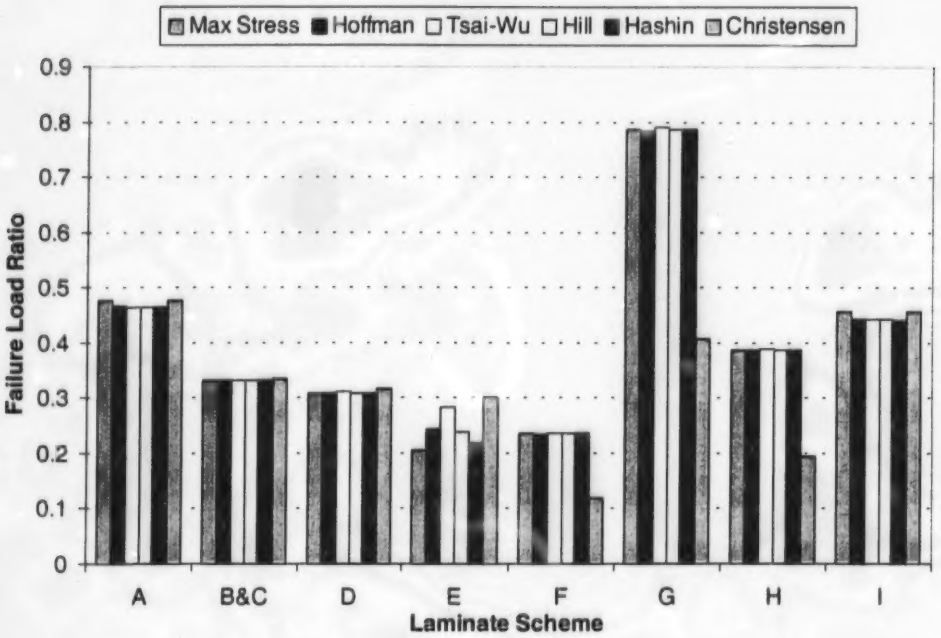

Figure 17: *Failure Load Ratios (Failure Load with Hole / Failure Load without Hole) for In-Plane Loading of Graphite Epoxy Laminates.*

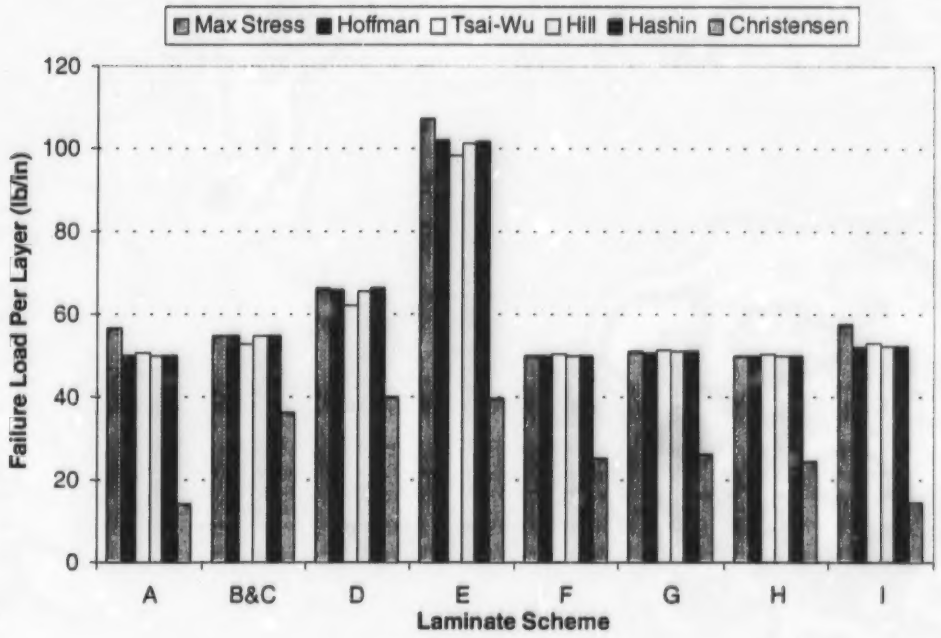

Figure 18: *Failure Loads Per Layer for In-Plane Loading of Graphite Epoxy Laminates with a Circular Hole.*

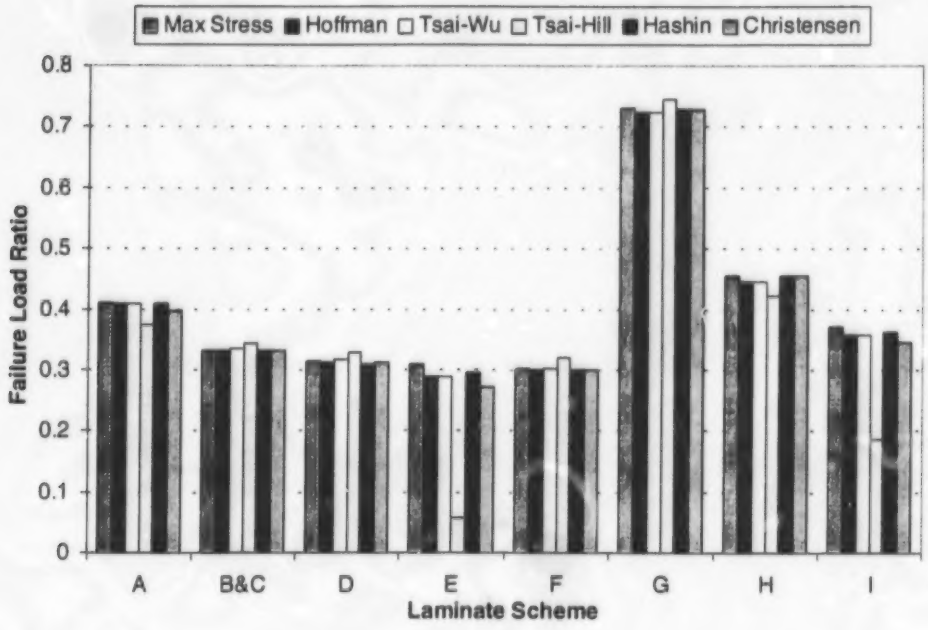

Figure 19: *Failure Load Ratios (Failure Load with Hole / Failure Load without Hole) for In-Plane Loading of Fibreglass Laminates.*

angle θ. Figure 21 shows the failure loads predicted with the Hashin criterion obtained with in-plane uniaxial loading of the 9×5 plate model. The failure is characterised by four distinct zones in which different failure modes occur. For θ between 0 and 11 degrees, the predicted failure is due to fibre breakage and the failure load remains approximately constant. Between 11 and 32 degrees the failure load drops rapidly to about 15 percent of its value at zero degrees. The matrix fails in compression in this region. This results from the component of the load perpendicular to the fibre direction exerting a compressive stress in the matrix. At 32 degrees the compressive failure gives way to an in-plane shear mode. In this region the failure load plateaus and then at 43 degrees begins to fall again. At about 50 degrees the shear mode gives way to a tensile matrix failure, as the matrix is now carrying most of the load. The failure load continues to fall until reaching a minimum at 90 degrees. The boundaries of the failure zones are virtually identical for the two-ply and four-ply laminates. As expected, the failure loads differ by a factor of two.

The analysis was repeated for the 9×5 plate model with a one inch diameter hole, the results of which are shown in Figure 22. The most notable differences in the failure behaviour occurs in the 0 to 20 degree range. At zero degrees the failure load is less than one-tenth that of the defect-free plate. The fibre breakage zone of the defect-free plate is replaced by a shear failure zone between 0 and 6 degrees and

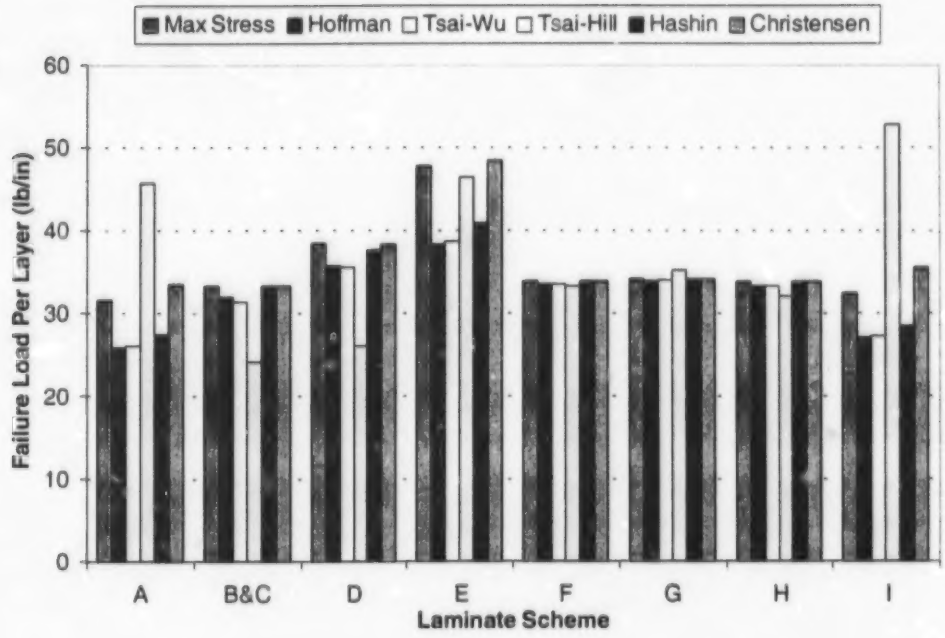

Figure 20: *Failure Loads Per Layer for In-Plane Loading of Fibreglass Laminates with a Circular Hole.*

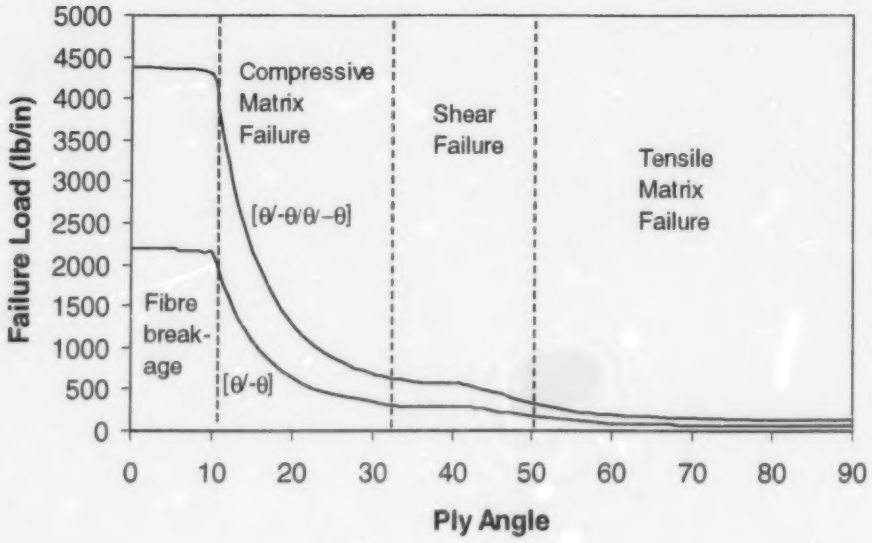

Figure 21: *Failure Loads as a Function of Ply Angle for a Uniform Plate with Two Angle-Ply Graphite Epoxy Laminates.*

a tensile matrix failure zone between 6 and 9 degrees. At ply angles of 9 degrees a compressive matrix failure mode begins, and thereafter the failure behaviour of the plate resembles that of the defect-free plate. In the shear failure mode that occurs between 32 and 50 degrees the failure load is reduced by a factor slightly more than two compared with the defect-free plate. In the tensile matrix failure zone that occurs for ply angles above 50 degrees, the failure load is reduced by a factor slightly more than 2.5 compared with the defect-free result. Evidently, the stress concentration due to the hole drastically reduces the strength of plies with orientations in the range 0 to 15 degrees, whereas it reduces the strength of other plies more moderately. Nonetheless, highest failure loads are obtained for plies of about ten degrees when there is a hole in the plate.

The same analysis was performed with fibreglass angle-ply laminates (Figures 23 and 24). The angular dependence of the failure load level and failure modes were found to be more simple than with Gr-Ep. Regions of compressive matrix failure are conspicuously absent from the failure diagram, due to the greater strength of the material in the -2 direction. The fibre breakage region is somewhat smaller in the defect-free plate, and there is no plateau at small angles of away from zero degree alignment. Finally the region of shear failure is larger with fibreglass than with Gr-Ep, partly as a result of the absence of a compressive failure region, and partly due to lower shear strengths.

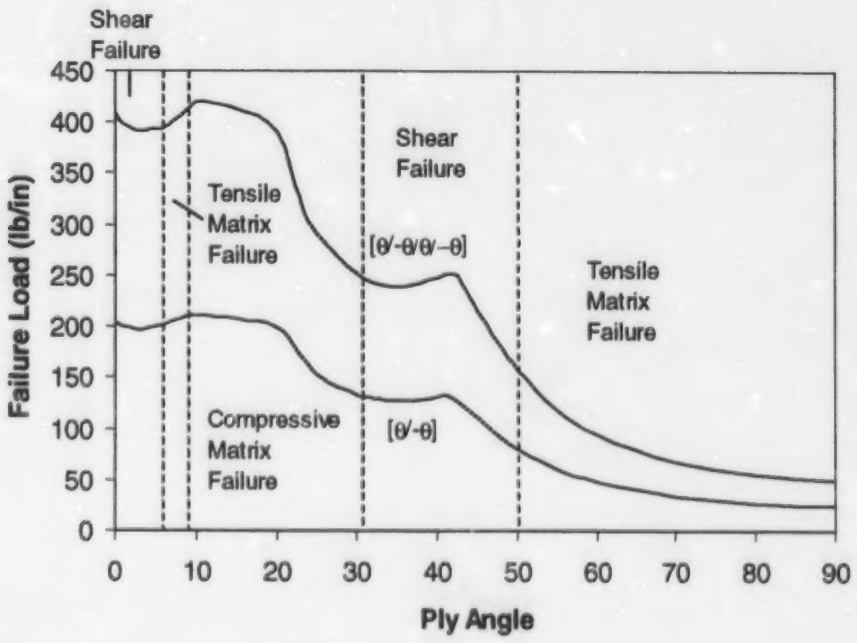

Figure 22: *Failure Loads as a Function of Ply Angle for a Plate with a Hole and with Two Angle-Ply Graphite Epoxy Laminates.*

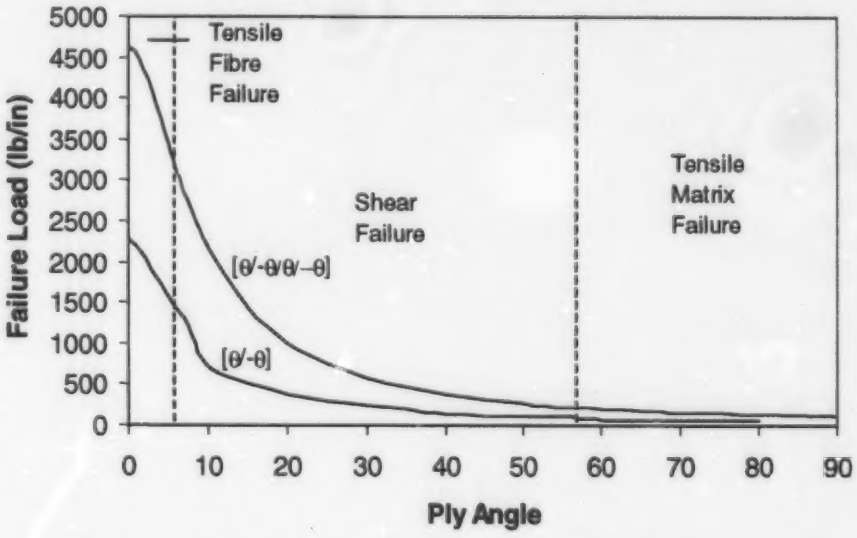

Figure 23: *Failure Loads as a Function of Ply Angle for a Uniform Plate with Two Angle-Ply Fibreglass Laminates.*

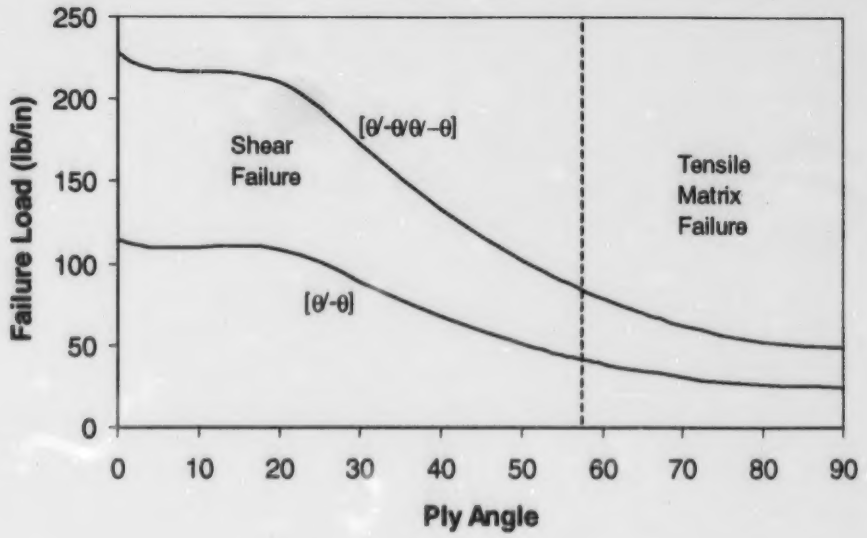

Figure 24: *Failure Loads as a Function of Ply Angle for a Plate with a Hole and with Two Angle-Ply Fibreglass Laminates.*

5 Summary and Concluding Remarks

The results of six stress-based macroscopic failure criteria have been compared in this study for nine different laminate schemes and two material types. The results have been obtained for a rectangular plate with uniform normal and in-plane loading, and in the latter case both with and without a stress concentration introduced in the form of a circular hole. Cross-ply, angle-ply, and quasi-isotropic laminate configurations have been included in the numerical tests. Also, the angular dependence on failure load in two and four-layer angle-ply laminates have been investigated.

Throughout these investigations, no one failure criterion has stood out as superior to the others. Two criteria (Tsai-Hill and the Christensen stress criterion) have proven to be unreliable. The Tsai-Hill criterion does not perform well with materials with differing tensile and compressive strengths due to the absence of first-order terms in the polynomial expression. The Christensen criterion uses assumptions about the strength values that may not be consistent with the actual material data. The other four criteria (Maximum Stress, Hoffman, Tsai-Wu and Hashin) have produced results that are generally consistent with one another. Minor discrepancies were observed in the Maximum Stress criterion for angle-ply laminates, and in Tsai-Wu criterion for some of the angle-ply and quasi-isotropic cases. Some differences are also observed between them in the predicted failure location and mode of failure. Overall, the Hoffman and Hashin criteria appear to be the most reliable. However,

there does not appear to be any clear advantage to using a piecewise "mode-based" criteria instead of a polynomial-based criteria. The mode-based criterion of Hashin and polynomial criterion of Hoffman predicted similar failure loads, failure locations and modes of failure, overall.

The most common mode of failure predicted among all the criteria was tension failure in 2 direction (perpendicular to the fibres for unidirectional laminae). Normally this indicates a matrix failure, but this conclusion should be viewed with scepticism. Hart-Smith [10] has pointed out that it does not make sense to design a laminate containing expensive fibres to fail in its inexpensive resin, and in practice well designed laminates do not do so. The repeated prediction of matrix-related failure in quasi-isotropic laminates is more likely indicative of some other effect. This may include inaccurate stiffness and strength data, unrealistic loads or constraints, and the presence of some other unmodelled failure mechanism, such as delamination.

Another possibility is that stress-based failure criteria are inappropriate for the types of failure they are trying to predict. It has to be emphasized that the use of homogenised stresses in the criteria is a computational convenience. By using these stresses the tendency is to underestimate the fibre stresses, since the load in the fibre direction is assumed to be carried by the whole sectional area of a ply. It is not possible to say whether the homogenised stress over- or under-estimates the real stress in the matrix. The stress field normal to the fibres is very complicated, due to stress concentrations introduced by the presence of the fibres, as well as by voids and microcracking. The most likely failure scenerios are cracking of the matrix in the vicinity of stress concentrations, or separation of the matrix from the fibres. Neither of these can be predicted with homogenised stresses.

One may also question the importance of localised matrix failures. The relatively small amount of load carried by the matrix could, in the event of a failure, be easily absorbed by surrounding layers with fibres in the loading direction. The purpose of the matrix is to provide internal and overall lateral stability to the laminate while the fibres carry the load. In this sense, a first-ply failure approach does not distinguish between significant and insignificant failures in a laminate, as it is incapable of assessing its residual load-bearing capacity following a failure. The implication of this is that the first-ply approach may give overly conservative estimates of failure loads in situations where a matrix failure is predicted, and for this reason, it is important to consider both the mode of failure and the failure load. A more realistic modelling of the failure process would be obtained with a progressive failure approach in combination with non-linear FEA. Micro-mechanical analysis might also be used to investigate how small scale defects affect the strength of the material.

References

1. Zhu, H., Sankar, B. V., and Marrey, R.V. (1998). Evaluation of Failure Criteria for Fiber Composites Using Finite Element Micromechanics. *Journal of Composite Materials,* 32 (8), 766–782.

2. Garnich, M. R., and Hansen, A. C. (1997). A Multicontinuum Approach to Structural Analysis of Linear Viscoelastic Composite Materials. *Journal of Applied Mechanics,* 64 (4), 795–803.

3. Skudra, A. M. (1985). Micromechanics of Failure of Reinforced Plastics. In G. C. Sih and A. M. Skudra (Eds.), *Failure Mechanics of Composites,* pp. 1–69. Amsterdam, The Netherlands: Elsevier Science Publishers.

4. Rowlands, R. E. (1985). Strength (Failure) Theories and their Experimental Correlation. In G. C. Sih and A. M. Skudra (Eds.), *Failure Mechanics of Composites,* pp. 71–125. Amsterdam, The Netherlands: Elsevier Science Publishers.

5. Nahas, M. N. (1986). Survey of Failure and Post-Failure Theories of Laminated Fiber-Reinforce Composites. *Journal of Composite Technology & Research,* 8 (4, 138–153.

6. Echaabi, J., Trochu, F., and Gauvin, R. (1996). Review of Failure Criteria of Fibrous Composite Materials. *Polymer Composites,* 17 (6), 786–796.

7. Tsai, S. W. (1965). Strength Characteristics of Composite Materials. (NASA CR-224). National Aeronautics and Space Administration.

8. Hoffman, O. (1967). The Brittle Strength of Orthotropic Materials. *Journal of Composite Materials,* 1, 200–206.

9. Tsai, S. W., and Wu, E. M. (1971). A General Theory of Strength for Anisotropic Materials. *Journal of Composite Materials,* 5, 58–80.

10. Hart-Smith, L. J. (1992). How to Calculate In-Plane Strengths of Fiber-Polymer Composite Laminates. *SAMPE Journal,* 28(6) 25–35.

11. Tennyson, R. C., MacDonald, D., and Nanyaro, A. P. (1978). Evaluation of the Tensor Polynomial Failure Criterion for Composite Materials. *Journal of Composite Materials,* 12, 63–75.

12. Pang, S.-S., Pandian, A., and Bradshaw, R. D. (1992). Modified Tsai-Wu Failure Criterion for Fiber-Reinforced Composite Laminates. *Polymer Composites,* 13(4) 273–277.

13. Hashin, Z. (1980). Failure Criteria for Unidirectional Fiber Composites. *Journal of Applied Mechanics,* 47(3), 329–334.

14. Hart-Smith, L. J. (1990). A Strain-Based Maximum Shear Stress Failure Criterion for Fibrous Composites. In *Proceedings of the AIAA/ASME/ASCE/AHS/ASC 31st Structures, Structural Dynamics and Materials Conference,* 714–722. American Institute of Aeronautics and Astronautics.

15. Christensen, R. M. (1988). Tensor Transformations and Failure Criteria for the Analysis of Fiber Composite Materials. *Journal of Composite Materials,* 22, 874–897.

16. Christensen, R. M. (1997). Stress Based Yield/Failure Criteria for Fiber Composites. *International Journal of Solids and Structures,* 34(5), 529–543.

17. Feng, W. W. (1991). A Failure Criterion for Composite Materials. *Journal of Composite Materials,* 25, 88–100.

18. Yeh, H.-Y., and Kim, C. H. (1994). The Yeh-Stratton Criterion for Composite Materials. *Journal of Composite Materials,* 28(10), 926–939.

19. Labossiere, P., and Neale, K. W. (1988). A General Strength Theory for Orthotropic Fiber-Reinforced Composite Laminae. *Polymer Composites,* 9(5), 306–317.

20. Neale, K. W., and Labossiere, P. (1989). Failure of Composite Laminae Under Biaxial Loading. *Polymer Composites,* 10(5), 285–292.

21. Makinde, A., Neale, K. W., and Sacharuk, Z. (1992). A Strain-Based Parametric Biaxial Failure Criterion for Fiber-Reinforced Composites. *Polymer Composites,* 13(4), 263–272.

22. Echaabi, J., Trochu, F., Gauvin, R. (1995). A General Strength Theory for Composite Materials Based on Dual Kriging Interpolation. *Journal of Reinforced Plastics and Composites,* 14, 211–232.

23. Reddy, J. N., and Pandey, A. K. (1987). A First-Ply Failure Analysis of Composite Laminates. *Computers & Structures,* 25 (3), 371–393.

24. Smith, M. J. (2000). A Flat-Facet Quadrilateral Element for Linear Elastic Analysis of Laminated Composite Plates and Shells. (DREA TM 1999-210). Defence Research Establishment Atlantic.

List of symbols, abbreviations, acronyms and initialisms

C_{ij}	laminar stiffness coefficients
F_i, F_{ij}	tensor coefficients
FEA	finite element analysis
FELAM	Finite Element Analysis of Laminates
FRP	fibre-reinforced plastic
Gr-Ep	graphite epoxy
MASTSAS	Mast Structural Analysis System
s_1^+, s_2^+, s_3^+	tensile normal strain limits of a lamina
s_1^-, s_2^-, s_3^-	compressive normal strain limits of a lamina
s_4, s_5, s_6	shear strain limits of a lamina
S_1^+, S_2^+, S_3^+	tensile normal strengths of a lamina
S_1^-, S_2^-, S_3^-	compressive normal strengths of a lamina
S_4, S_5, S_6	shear strengths of a lamina
u, v, w	displacement variables in Cartesian coordinates
ϵ_1, ϵ_2, ϵ_3	normal strain components in fibre coordinates
ϵ_4, ϵ_5, ϵ_6	shear strain components in fibre coordinates
σ_1, σ_2, σ_3	normal stress components in fibre coordinates
σ_4, σ_5, σ_6	shear stress components in fibre coordinates
ψ_x, ψ_y, ψ_z	rotation variables about Cartesian axes

Annex A
Sample Felam Model File

```
#Nodes 9
#Elements 4
#Materials 2
node 0  0     0    0
node 1  2.25  0    0
node 2  4.5   0    0
node 3  0     1.25 0
node 4  2.25  1.25 0
node 5  4.5   1.25 0
node 6  0     2.5  0
node 7  2.25  2.5  0
node 8  4.5   2.5  0
material 0 OrthoElastic {
      name T300/5208
      E11  19.2e+06
      E22  1.56e+06
      G12  0.82e+06
      G13  0.82e+06
      G23  0.49e+06
      pr12 0.24
      density 0.0
      failureTheory  Hashin {
           tensile11          219.5e+03
           compression11      246.0e+03
           tensile22          6.35e+03
           compression22      6.35e+03
           tensile33          6.35e+03
           compression33      6.35e+03
           shear12            12.6e+03
           shear13            12.6e+03
           shear23            9.8e+03
}
}
material 1 ThickLaminate {
      name [0/90]
      shearDeformation
      layer {
```

```
            materialIndex       0
            thickness           0.005
            orientation         0.0
      }
      layer {
            materialIndex       0
            thickness           0.005
            orientation         90.0
      }
}
element 0 QuadShell {
      nodes 0 1 4 3
      materialIndex 1
      propertyIndex 0
      orientation 0
}
element 1 QuadShell {
      nodes 1 2 5 4
      materialIndex 1
      propertyIndex 0
      orientation 0
}
element 2 QuadShell {
      nodes 3 4 7 6
      materialIndex 1
      propertyIndex 0
      orientation 0
}
element 3 QuadShell {
      nodes 4 5 8 7
      materialIndex 1
      propertyIndex 0
      orientation 0
}
```

UNCLASSIFIED
SECURITY CLASSIFICATION OF FORM
(highest classification of Title, Abstract, Keywords)

DOCUMENT CONTROL DATA

(Security classification of title, body of abstract and indexing annotation must be entered when the overall document is classified)

1. ORIGINATOR (the name and address of the organization preparing the document.. Organizations for whom the document was prepared, e.g. Establishment sponsoring a contractor's report, or tasking agency, are entered in section 8.)

Defence Research Establishment Atlantic
PO Box 1012
Dartmouth, Nova Scotia, Canada B2Y 3Z7

2. SECURITY CLASSIFICATION (overall security classification of the document including special warning terms if applicable).

UNCLASSIFIED

3. TITLE (the complete document title as indicated on the title page. Its classification should be indicated by the appropriate abbreviation (S,C,R or U) in parentheses after the title).

First-Ply Failure Prediction of Fibrous Composites with Finite Element Analysis

4. AUTHORS (Last name, first name, middle initial. If military, show rank, e.g. Doe, Maj. John E.)

Smith, Malcolm J.

5. DATE OF PUBLICATION (month and year of publication of document)	6a. NO .OF PAGES (total containing information Include Annexes, Appendices, etc).	6b. NO. OF REFS (total cited in document)
June 2001	62	24

7. DESCRIPTIVE NOTES (the category of the document, e.g. technical report, technical note or memorandum. If appropriate, enter the type of report, e.g. interim, progress, summary, annual or final. Give the inclusive dates when a specific reporting period is covered).

TECHNICAL MEMORANDUM

8. SPONSORING ACTIVITY (the name of the department project office or laboratory sponsoring the research and development. Include address).

Defence Research Establishment Atlantic

9a. PROJECT OR GRANT NO. (if appropriate, the applicable research and development project or grant number under which the documeat was written. Please specify whether project or grant).	9b. CONTRACT NO. (if appropriate, the applicable number under which the document was written).
Project 1.g.c.11	

10a ORIGINATOR'S DOCUMENT NUMBER (the official document number by which the document is identified by the originating activity. This number must be unique to this document.)	10b OTHER DOCUMENT NOs. (Any other numbers which may be assigned this document either by the originator or by the sponsor.)
	DREA TM 2001-065

11. DOCUMENT AVAILABILITY (any limitations on further dissemination of the document, other than those imposed by security classification)

(X) Unlimited distribution
( ) Defence departments and defence contractors; further distribution only as approved
( ) Defence departments and Canadian defence contractors; further distribution only as approved
( ) Government departments and agencies; further distribution only as approved
( ) Defence departments; further distribution only as approved
( ) Other (please specify):

12. DOCUMENT ANNOUNCEMENT (any limitation to the bibliographic announcement of this document. This will normally correspond to the Document Availability (11). However, where further distribution (beyond the audience specified in (11) is possible, a wider announcement audience may be selected).

UNCLASSIFIED
SECURITY CLASSIFICATION OF FORM

13. ABSTRACT (a brief and factual summary of the document. It may also appear elsewhere in the body of the document itself. It is highly desirable that the abstract of classified documents be unclassified. Each paragraph of the abstract shall begin with an indication of the security classification of the information in the paragraph (unless the document itself is unclassified) represented as (S), (C), (R), or (U). It is not necessary to include here abstracts in both official languages unless the text is bilingual).

The usefulness of macroscopic failure theories for laminated composites is investigated by means of a finite element based approach for determining first-ply failure loads of structures. A review of phenomenological (macroscopic) failure theories is provided, with detailed descriptions of six stress-based theories. The computational approach for first-ply failure analysis uses a linear static finite element analysis, followed by the iterative scaling of the stress-strain results to satisfy the chosen failure criterion. The resulting scaling factor defines the failure load. The first-ply algorithm and failure criteria have been implemented in a special-purpose finite element code for laminated plate and shell structures. Failure loads are predicted and validated with the six selected stress-based criteria for a rectangular composite plate structure with transverse and in-plane loading. The effect of the stress concentration produced by a circular hole is then considered for the in-plane loading case. The strength of angle-ply laminates, both with and without a stress concentration, is then examined as a function of the ply angle. Although no one criterion stands out as superior to the others, good consistency is obtained by four out of the six criteria in predicting failure loads and locations. Among these four, the Maximum Stress and Tsai Wu criteria showed a tendency to over-predict the failure loads, especially with angle-ply laminates. The most consistently performing criteria in the examples tested were the Hoffman and Hashin criteria.

14. KEYWORDS, DESCRIPTORS or IDENTIFIERS (technically meaningful terms or short phrases that characterize a document and could be helpful in cataloguing the document. They should be selected so that no security classification is required. Identifiers, such as equipment model designation, trade name, military project code name, geographic location may also be included. If possible keywords should be selected from a published thesaurus. e.g. Thesaurus of Engineering and Scientific Terms (TEST) and that thesaurus-identified. If it not possible to select indexing terms which are Unclassified, the classification of each should be indicated as with the title).

Composite
Laminate
Fibre reinforced plastics
Failure criterion
Macroscopic failure theory
Phenomenological failure theory
First-ply failure
Finite element analysis
Quadrilateral shell element